HELMHOLTZ ZENTRUM DRESDEN ROSSENDORF

HELMHOLTZ-INSTITUT FREIBERG FÜR RESSOURCENTECHNOLOGIE

Neues Potential

First interim report

Jan Černý [1], Marie Guilcher[1], Sam Thiele[1], Mathias Burisch[1,2], Jens Gutzmer[1]

[1] Helmholtz-Zentrum Dresden-Rossendorf, Helmholtz Institute Freiberg for Resource Technology, Chemnitzer Straße 40, 09599 Freiberg, Germany

[2] Department of Geology and Geological Engineering, Colorado School of Mines, 1516 Illinois Street, Golden, CO, 80401, USA

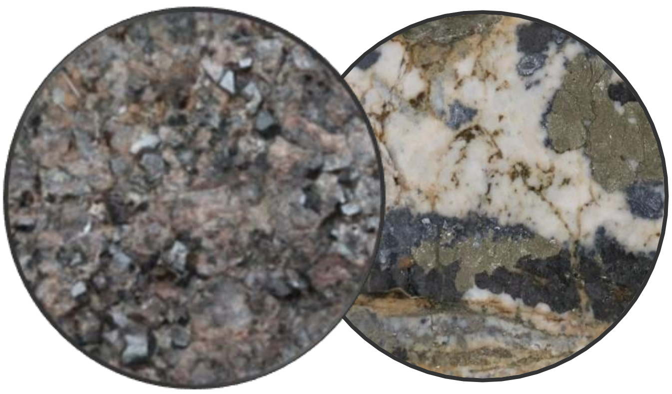

April 25th 2023, Freiberg

Table of Contents

List of Figures

List of Tables

1. Introduction

This document is the first internal report for the "Neues Potential" project in collaboration with the Sächsisches Landesamt für Umwelt, Landwirtschaft und Geologie (LfULG). This two-year project will develop a novel mineral systems model for the Eastern Erzgebirge (Germany) with a focus on magmatic-hydrothermal Li-Sn-W greisen, skarn and Ag-Pb-Zn vein-style mineralization related to late Variscan or post-orogenic granitoid intrusions. The results obtained will be used to constrain search space and to define exploration vectors for future mineral exploration in the Eastern Erzgebirge region.

In this internal report, we provide the status of the project and the progress of the six first months (from November 2022 to April 2023. The anticipated next steps for the upcoming six months are also presented.

The main tasks of the "Neues Potential" project include:

- acquisition and compilation of structural and geochemical data
- integration and synthesis of multiple approaches and datasets (field observations, petrography, structural analyses, fluid inclusion, geochronology)
- update on the geological overview of the magmatic and magmatic-hydrothermal systems, and essential knowledge gaps in the study area based on historic and new data
- building of a conceptual metallogenic model for the late-variscan magmatic and epithermal systems of the eastern Erzgebirge
- publication of new datasets as well as novel tectonic and metallogenetic concepts.

These tasks are organized into six work packages that constitute the structure of this internal report:

(1) Geochronology and geochemistry (work package 1): utilization of a wide range of analytical tools (e.g., microthermometry, LA-ICP-MS) to clarify the genetic relationship of diverse ore deposit types such as greisen and Ag-Pb-Zn epithermal veins. For this purpose, a wide selection of samples from historic geoscientific collections, exploration companies drill cores and surface outcrops are investigated in order to cover as much as possible the study area.

(2) Structural and tectonic interpretation (work package 2): a structural geological and tectonic interpretation will be developed by synthesis of available datasets and

integration of new geochronology data to provide a conceptual structural framework for ore deposit genesis.

(3) Development of an integrated mineral system (work packages 3 to 5): The development of one or more hypothesis(es) on the source, transport paths, and traps for ore deposits using the mineral systems framework.

(4) Publication and dissemination (Work Package 6): results will be made available via the publication in “open access” peer-review journals and LfULG scientific publications.

2. WP 1 - Geochronology and geochemistry

Disentangling the sequence of mineralising events, and the spatio-temporal relationship between the magmatic and epithermal mineral systems, is key to the development of a comprehensive mineral system model for the Eastern Erzgebirge. This work package aims to review and collect new geochronology, mineral chemistry and fluid inclusion data to address these questions.

2.1. Current progress

2.1.1. Data compilation and identified knowledge gaps

Literature research was carried out to compile the geochronological data previously published in German and international scientific literature up to the present day (April 2023). Ages for the East Erzgebirge are compiled in the Appendix 1. Literature research illustrates an abundance of radiometric age data for many of the granitic and rhyolitic rocks of the Eastern Erzgebirge region, but also some very obvious gaps, for example, no radiometric age appears to be available for the Schellerhau granite in the central part of the Altenberg-Teplice caldera. Furthermore, there is only one rather poorly constrained age of 278±20 Ma (Rb-Sr on sphalerite) available for the Ag-Pb-Zn epithermal veins in the Freiberg district (Ostendorf et al., 2019). Although this age is deemed robust, its large error does not allow for confident correlation of vein formation with regional magmatic systems. Multiple ages are available for the Sn-Li-greisen deposits inside or in the vicinity of the Altenberg-Teplice caldera, but some of these are conflicting – and not in agreement with field geological evidence. The above illustrates that the acquisition of additional ages for the mineral deposits and magmatic rocks of the Eastern Erzgebirge is needed. In the focus of the present study is the age-dating of smaller greisen occurrences and veins that will help better constrain the timing of ore deposits in the study region.

2.1.2. Sample acquisition and preparation

A selection of ~50 samples were gathered from the TUBAF mineral collection, LfULG archives and recent Excellon drill cores. Of these, 32 were chosen to constitute a first batch of samples for geochronology (Tables 2-1 and 2-2). From the Ag-Pb-Zn epithermal veins of the Freiberg and Meißen districts, 16 samples hosting carbonates (e.g., dolomite-ankerite, Mn-bearing calcite, rhodochrosite) were selected. The localities sampled are Kleinvoigtsberg, Reinsberg, Brand-Erbisdorf, Bräunsdorf, Grauer Wolf, Zug, Reichenbach and Halsbrücke near Freiberg and Scharfenberg near Meißen (Fig. 2-1). These samples are mainly from previous Ph.D and M.Sc. projects, so their mineral paragenesis and association with mineralization is well documented. From Sn-greisen bodies and associated Sn-quartz veins, 16 samples were selected from historic mining districts of Zinnwald, Altenberg, Bärenfels, Niederpöbel, Lauenstein, Schmiedeberg, Panorama Höhe, Sachsenhöhe and Krupka. The sampling locations are illustrated in Figure 2-1.

Table 2-1. Cassiterite-bearing samples of Sn greisen and veins from the surrounding of the Altenberg-Teplice caldera and cassiterite-bearing samples of the Ag-Pb-Zn epithermal veins of the Freiberg district.

Sample ID	Depth	District	Subdistrict	Mineralogy	Host-rock	Collection
MG_Znn_66533		Zinnwald	Zinnwald	Cassiterite, wolframite	Altered granite	TUBAF
65775		Altenberg	Altenberg	Coarse tin concentrate	Altered granite	TUBAF
MG_Znn_43652		Zinnwald	Zinnwald	Cassiterite, zinnwaldite, quartz	Altered granite	TUBAF
MG_Znn_43672		Zinnwald	Zinnwald	Cassiterite, zinnwaldite	Altered granite	TUBAF
MG_Znn_43697		Zinnwald	Zinnwald	Cassiterite, wolframite	Altered granite	TUBAF
MG_Znn_43659		Zinnwald	Zinnwald	Cassiterite (massive, smooth surfaces), zinnwaldite, quartz	Altered granite	TUBAF
CRFG4		Freiberg	Kleinvoigtsberg*	Pyrite, proustite, galena, quartz, cassiterite		TUBAF
MG_HB_51003		Freiberg	Halsbrücke	Cassiterite (?), galena		TUBAF
MG_BA_66818			Bärenfels	Cassiterite		TUBAF
43245				Wolframite, cassiterite	Altered granite	TUBAF
MG_SK_SS18875			Lauenstein	Cassiterite		LfULG
MG_SC_SS4024			Schmiedeberg	Cassiterite in quartz vein	Altered granite	LfULG
MG_KP_RS8653		Krupka	Krupka	Cassiterite		LfULG
MG_NDP_66044			Niederpöbel	Cassiterite, quartz		TUBAF
14-23b			Sadisdorf	wolframite		TUBAF

65803	Altenberg	Altenberg**	Cassiterite	TUBAF

* Alte Hoffnung Gottes mine

** Zinnklüfter vein, „Zwitterstocks tiefen Erbstolln“

Table 2-2. Carbonate-bearing samples from Ag-Pb-Zn epithermal veins of the Freiberg and Meißen districts.

Sample ID	District	Subdistrict	Description	Mineralogy	Host-rock	Collection
52924A	Freiberg	Reinsberg	Emanuel Erbstolln, Reinsberger Glück Morgengang, über 4. Gezeugstrecke in Nordost	Quartz, carbonate, proustite/pyrargyrite, pyrite		TUBAF
LSFG024	Freiberg	Kleinvoigtsberg	Alte Hoffnung Gottes, Heinrich Stehender	Ag-Sb-sulfides, quartz		TUBAF
51538b	Freiberg	Brand-Erbisdorf	Himmelsfürst Fundgrube, Jupiter Stehender, 3. Gezeugstrecke, aus 1. Benjaminschacht in Süd	Galena, sphalerite, pyrite, ankerite, quartz	Gneiss	TUBAF
MG_BRD_01_353.30_1	Freiberg	Bräunsdorf		Quartz, carbonate, arsenopyrite, pyrite		EXCELLON
MG_GWO_030_272.65_1	Freiberg	Grauer Wolf		Quartz, carbonate, arsenopyrite, pyrite		EXCELLON
MG_REI_027_179.10_1	Freiberg	Reichenbach		Quartz, carbonate, arsenopyrite, pyrite		EXCELLON
MG_GWO_038_78.66_1	Freiberg	Grauer Wolf		Quartz, carbonate, arsenopyrite, pyrite		EXCELLON
MG_GWO_038_61.15_1	Freiberg	Grauer Wolf		Calcite (normal fault infill)		EXCELLON
MG_GWO_038_48.0_1				Quartz, carbonate, arsenopyrite, pyrite		
MG_GWO_040_392.8_1						
MG_KVB_52712	Freiberg	Kleinvoigtsberg	Alte Hoffnung Gottes Erbstolln, Frisch Glück Stehender, 32 Lachter vom Gottliebschacht in Süd	Galena, pyrite, carbonate		TUBAF
MG_SFB_53248	Meissen	Scharfenberg				TUBAF
52936B	Freiberg	Reinsberg	Emanuel Erbstolln, Reinsberger Glück	Quartz, carbonate,		TUBAF

			Morgengang, hartes Trum	chalcopyrite, acanthite		
MG_Z_WSt1	Freiberg	Zug	Wilhelm Stehender (Baustelle)	Sulfides, quartz, carbonate		Jens Gutzmer private collection
MG_BE_50881	Freiberg	Brand-Erbisdorf	Habacht Fundgrube, Hangendes Trum des Ludwig Stehenden bei 1. Gezeugstrecke, 90 Lachter vom Jung Schwarzfärber Spat in Nord	Boulangerite, galena, sphalerite, owyheeite, rhodocrosite, quartz		TUBAF
MG_BE_51145	Freiberg	Brand-Erbisdorf	Vergnügte Anweisung Fundgrube samt Reussen Fundgrube, Friedrich Stehender (carbonate breccia)	Galena, ankerite, calcite, pyrite, quartz	Gneiss	TUBAF

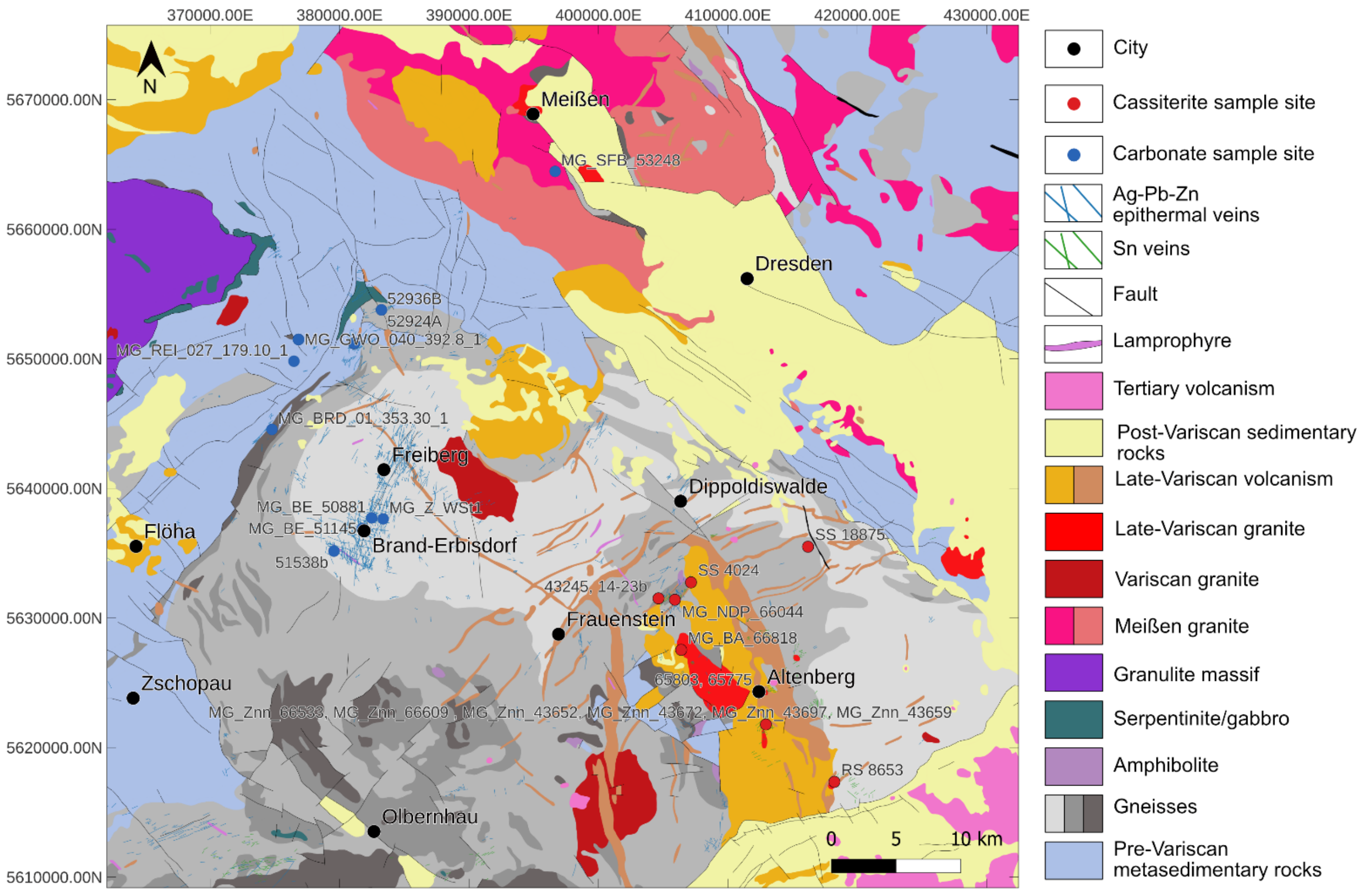

Figure 2-1. Sampling strategy for carbonates (in blue) and cassiterites (in red) from Ag-Pb-Zn epithermal vein and greisen bodies and veins. Simplified geological map modified after Hoth et al. (1980).

2.1.3. Geochronological measurements

The first batch of 32 samples was analysed on the 15 and 16 of December 2022 at the FIERCE laboratory at the Goethe University in Frankfurt (Germany). The U-Pb datation by La-ICP-MS is a method that has been successfully developed and used over the last decade on a large variety of minerals (e.g., garnet; Burisch et al., 2019a; Reinhardt et al., 2022). The specificity of this method is that it can be applied to low-U mineral phases such as carbonate (Burisch et al., 2017; Roberts et al., 2020; Guilcher et al., 2021). Results are expected within the next few months and will be reported in the next interim report.

2.1.4. Development of integrated time-space tectonic diagram

The ages compiled from published literature for magmatism, volcanism and ore deposits in the eastern part of the Erzgebirge are presented in Figure 2-2. This will be progressively updated over the course of the project, as new data become available.

2.2. Current challenges

Several difficulties were encountered during the initial stages of this study. These are reported below for reference.

1. There is an obvious lack of suitable sample material in accessible collections and archives for many of the smaller vein deposits in the Eastern Erzgebirge. Minor Ag-Pb-Zn veins are reported by Baumann (1965) near Sayda, Reichenau, Frauenstein, Schönfeld, Naundorf, Dippoldiswalde and Edle Krone (Fig. 2-3). Yet, no sample material from these sites is available. Therefore, no samples could be included in the first batch of samples for geochronology. Sampling from dumps, outcrops or visitor mines will be carried out in the coming months for geochronology and fluid inclusion study purposes.

2. For the greisen deposits, samples from the LfULG hand specimens collection for the localities of Bärenstein, Glashütte, Lauenstein, Schönfeld and Dippoldiswalde mostly consist of non-mineralized greisen samples. Samples from these localities in the TU Bergakademie Freiberg geoscientific collection are scarce. Additionally, no greisen samples were collected from the Falkenhain district because access to potential sample material was not provided by Deutsche Lithium GmbH.

3. An extensive search was conducted for cassiterite-bearing samples from the Pb-Zn-Ag epithermal veins in the Freiberg district to complement our attempt to date carbonate veins (as carbonates often do not give robust ages). Baumann (1965) reported euhedral cassiterite crystal in several samples from thin sections that are now stored in the ore deposit collection

of the TU Bergakademie Freiberg. However, up to today, no access to these thin sections has been provided by Prof. Thomas Seifert (currently responsible for the collections). Instead, we are actively reaching out to museums and private collectors to find suitable alternative cassiterite samples.

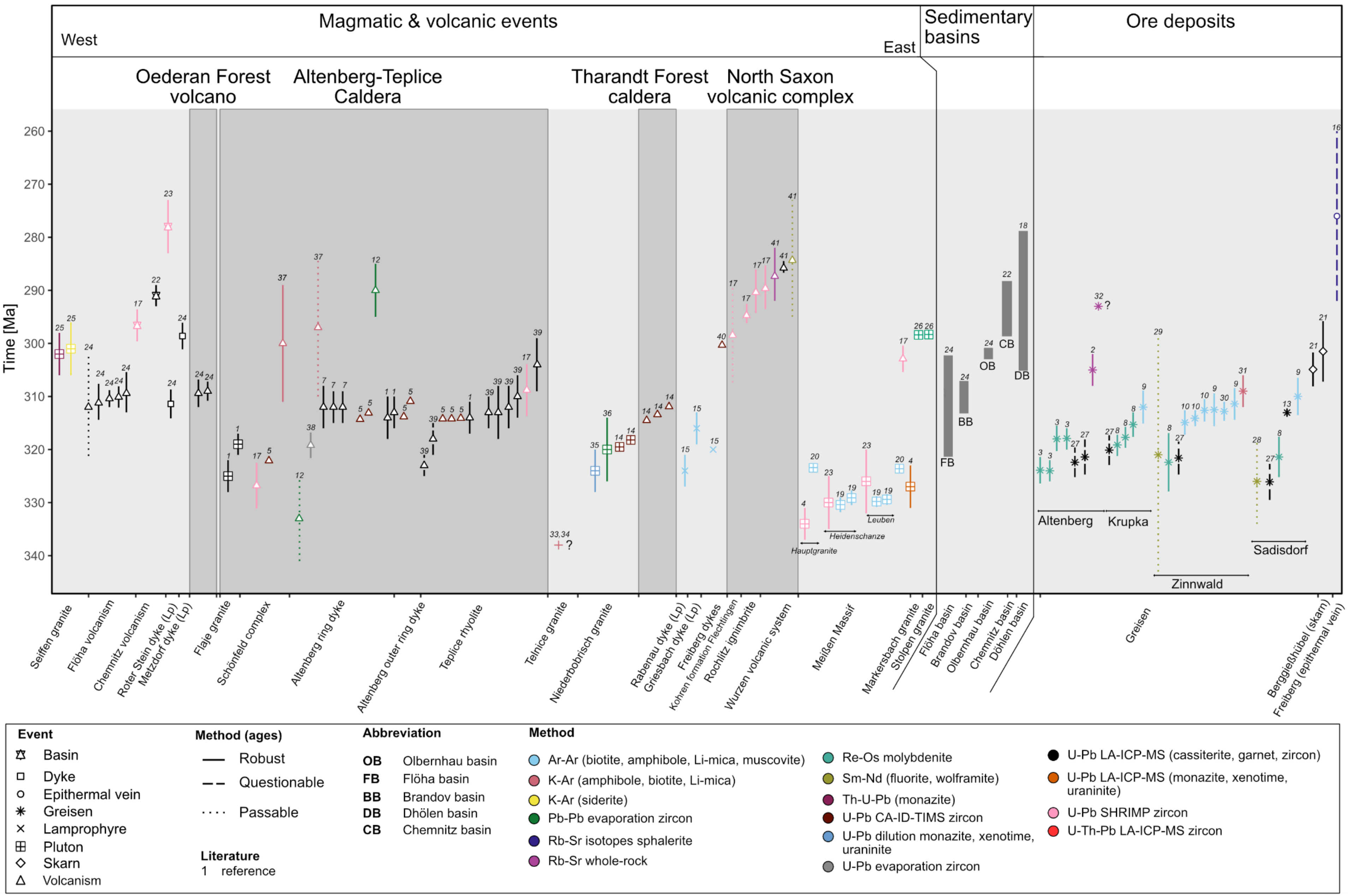

Magmatic & volcanic events
West
East
Sedimentary basins
Ore deposits
Oederan Forest volcano
Altenberg-Teplice Caldera
Tharandt Forest caldera
North Saxon volcanic complex
Time [Ma]
260
270
280
290
300
310
320
330
340
FB
BB
OB
CB
DB
Hauptgranite
Heidenschanze
Leuben
Altenberg
Krupka
Zinnwald
Sadisdorf
Seiffen granite
Flöha volcanism
Chemnitz volcanism
Roter Stein dyke (Lp)
Metzdorf dyke (Lp)
Flaje granite
Schönfeld complex
Altenberg ring dyke
Altenberg outer ring dyke
Teplice rhyolite
Telnice granite
Niederbobritsch granite
Rabenau dyke (Lp)
Griesbach dyke (Lp)
Freiberg dykes
Kohren formation Flechtingen
Rochlitz ignimbrite
Wurzen volcanic system
Meißen Massif
Markersbach granite
Stolpen granite
Flöha basin
Brandov basin
Olbernhau basin
Chemnitz basin
Döhlen basin
Greisen
Berggießhübel (skarn)
Freiberg (epithermal vein)
Event
Basin
Dyke
Epithermal vein
Greisen
Lamprophyre
Pluton
Skarn
Volcanism
Method (ages)
Robust
Questionable
Passable
Literature
1 reference
Abbreviation
OB Olbernhau basin
FB Flöha basin
BB Brandov basin
DB Dhölen basin
CB Chemnitz basin
Method
Ar-Ar (biotite, amphibole, Li-mica, muscovite)
K-Ar (amphibole, biotite, Li-mica)
K-Ar (siderite)
Pb-Pb evaporation zircon
Rb-Sr isotopes sphalerite
Rb-Sr whole-rock
Re-Os molybdenite
Sm-Nd (fluorite, wolframite)
Th-U-Pb (monazite)
U-Pb CA-ID-TIMS zircon
U-Pb dilution monazite, xenotime, uraninite
U-Pb evaporation zircon
U-Pb LA-ICP-MS (cassiterite, garnet, zircon)
U-Pb LA-ICP-MS (monazite, xenotime, uraninite)
U-Pb SHRIMP zircon
U-Th-Pb LA-ICP-MS zircon

Figure 2-2. Time-Space diagram compiling all ages available classified by the dating method used. References: 1. Tomek et al. (2021), 2. Gerstenberger et al. (1989), 3. Romer et al. (2007), 4. Hofmann et al. (2009), 5. Tichomirowa et al. (2022), 6. Opluštil et al. (2016), 7. Tomek et al. (2019), 8. Akerman et al. (2017), 9. Seifert et al. (2016), 10. Seifert et al. (2011), 11. Atanasova et al. (2012), 12. Kempe et al. (1999), 13. Leopardi et al. (*submitted*), 14. Breitkreuz et al. (2021), 15. Von Seckendorff et al. (2004), 16. Ostendorf et al. (2019), 17. Hoffmann et al. (2013), 18. Zieger et al. (2019), 19. Wenzel et al. (1997), 20. Sharp et al. (1997) in Müller (2011), 21. Burisch et al. (2019a), 22. Luthardt et al. (2018), 23. Nasdala et al. (1999), 24. Löcse et al. (2019), 25. Förster and Rhede (2006), 26. Käßner et al. (2021), 27. Zhang et al. (2017), 28. Kempe and Belyatsky (1997), 29. Höhndorf et al. (1994), 30. Neßler et al. (2016), 31. Dolejš and Štemprok (2001), 32. Haack (1990), 33. Štemprok et al. (2003), 34. Klomínský et al. (2010), 35. Förster et al. (1998), 36. Tichomirowa (1997), 37. Müller et al. (2005), 38. Romer et al. (2010), 39. Casas-Garcia et al. (2019), 40. Marion Tichomirowa (personal communication), 41. Wendt et al. (1995)

2.3. Next steps

The goals for the next six months are as follows:

A second batch of cassiterite from the Ag-Pb-Zn veins is being prepared to complement the carbonate dating of December 2022. The new batch of samples will be dated around August 2023 using the same method (U-Pb LA-ICP-MS).

Field work is scheduled to sample Ag-Pb-Zn veins located in the surrounding of the Altenberg-Teplice and the Tharandt caldera. New sampling is necessary to tackle the questions of fluid nature, paleodepth, and geochemistry of epithermal veins from other localities than Freiberg (e.g., Frauenstein, Edle Krone and other localities mentioned in section 2.2, Fig. 2-3). These areas have been identified as key knowledge gaps that potentially demarcate the boundary between the Freiberg and Altenberg-Teplice mineral systems.

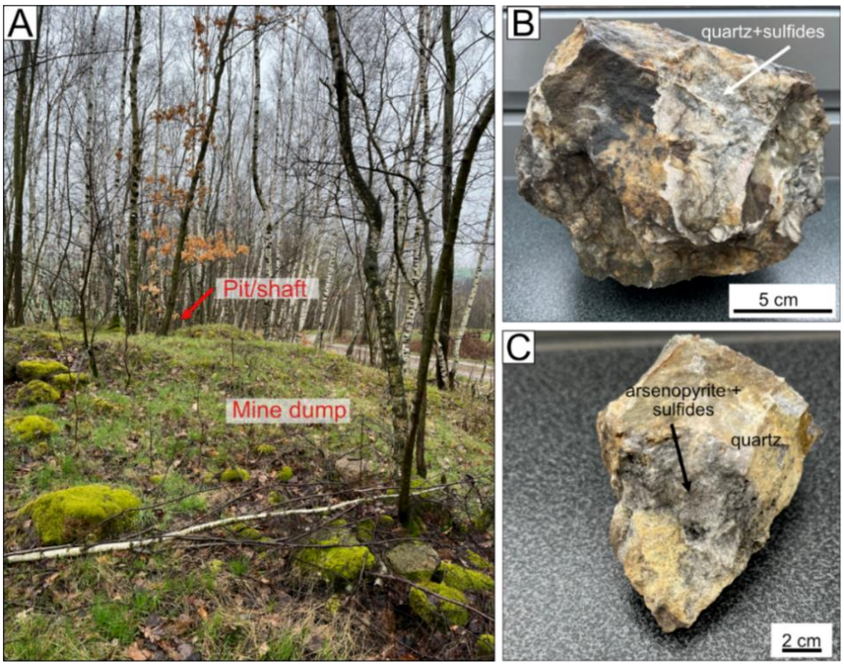

Figure 2-3. (A). Mine dump next to an abandoned pit/shaft in Mittelreichstädt (Fig. 2-4, near Reichstädt, Dippolsdilwalde district, coordinates UTM zone 33: 403482.4, 5634737.0) located on a Ag-Pb-Zn epithermal veins occurrence. (B-C). Samples collected from the mine dump.

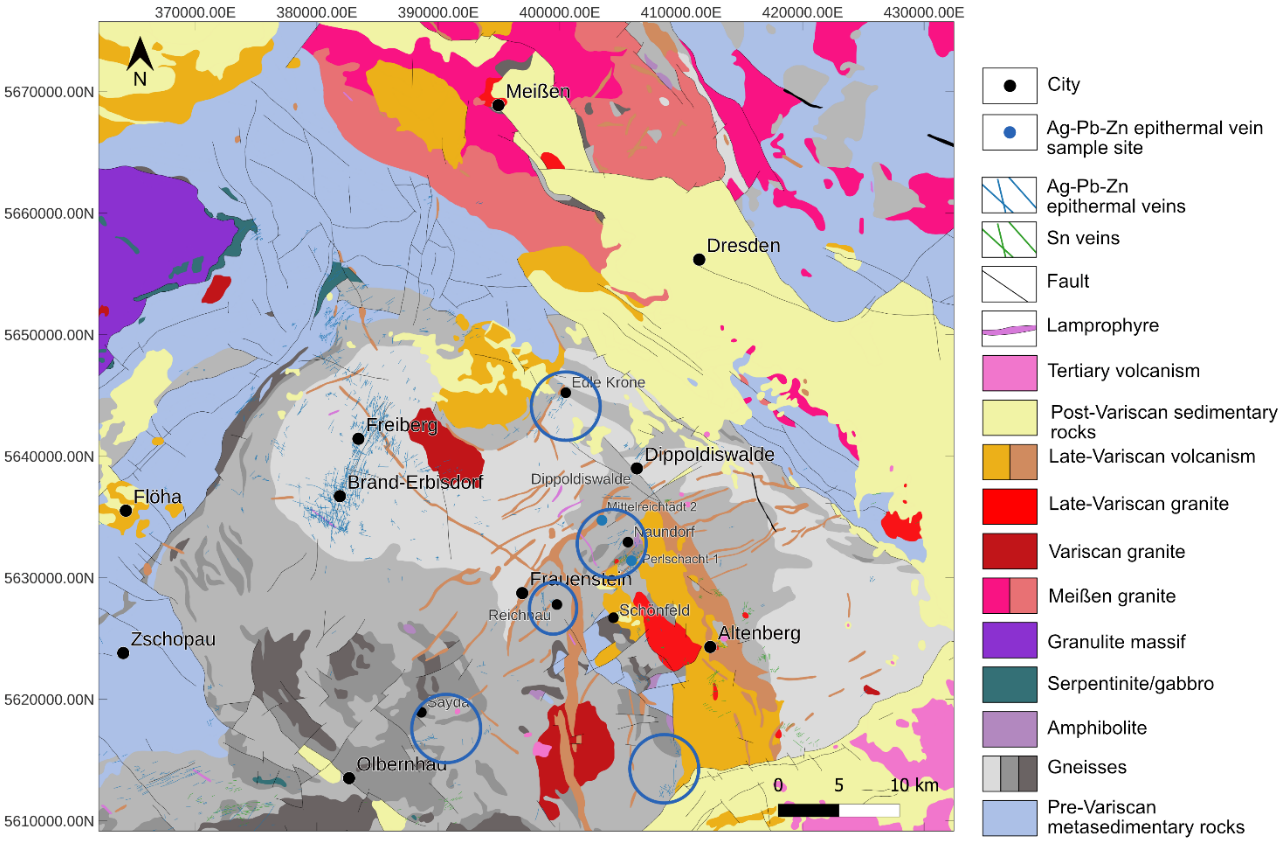

Figure 2-4. Sampling strategy for Ag-Pb-Zn epithermal veins for future geochronology and geochemistry/fluid inclusion analysis. Sampling is focused on districts in the surroundings of the Altenberg-Teplice caldera, Dippoldiswalde district and Tharandt caldera. Simplified geological map modified after Hoth et al. (1980).

3. WP 2 - Structure and Tectonics

Crustal and local-scale structures, and their interaction with the broader tectonic setting, are a key control on the localization of magmatic-hydrothermal ore deposits. This work package focuses on (1) reviewing the range of possible tectonic settings for the Eastern Erzgebirge mineral system, especially after the peak Variscan metamorphism, and (2) using mapped and inferred structures to provide geometric constraints on flow pathways that focused mineralizing magmas and fluids during post-Variscan mineralizing events. Potential links between magmatic and epithermal mineralization and the Tharandt and Altenberg-Teplice caldera systems will also be considered.

3.1. Current progress

3.1.1. Literature review and tectonic context

The Eastern Erzgebirge (EE) is a part of the Saxothuringian unit (STU), which outcrops along the Variscan belt and forms the northern margin of the Bohemian Massif. Over the last decades, diverse concepts for the evolution of the Saxuthuringian unit have been proposed. The structural complexity of the whole Bohemian Massif has led many authors to the conclusion that it resulted from several accretionary collisions between various microplates/terranes, however interpretations of the nature and timing of these collisions differ. These terranes consist of Upper Proterozoic to Upper Devonian rocks, and their geochemistry indicates different origins, including ocean floor (ophiolite), island arc, shelf, and active continental margin (e.g., Oliver et al., 1993). The first amalgamation has been suggested to have occurred along the Tornquist line, during the upper Ordovician time (~460–445 Ma), as some relics of Caledonian orogeny have been found in Poland (Oliver et al., 1993; Cymerman, 2000). The second suggested amalgamation coincides with Variscan orogenesis at Middle to Upper Devonian time (~390–360 Ma).

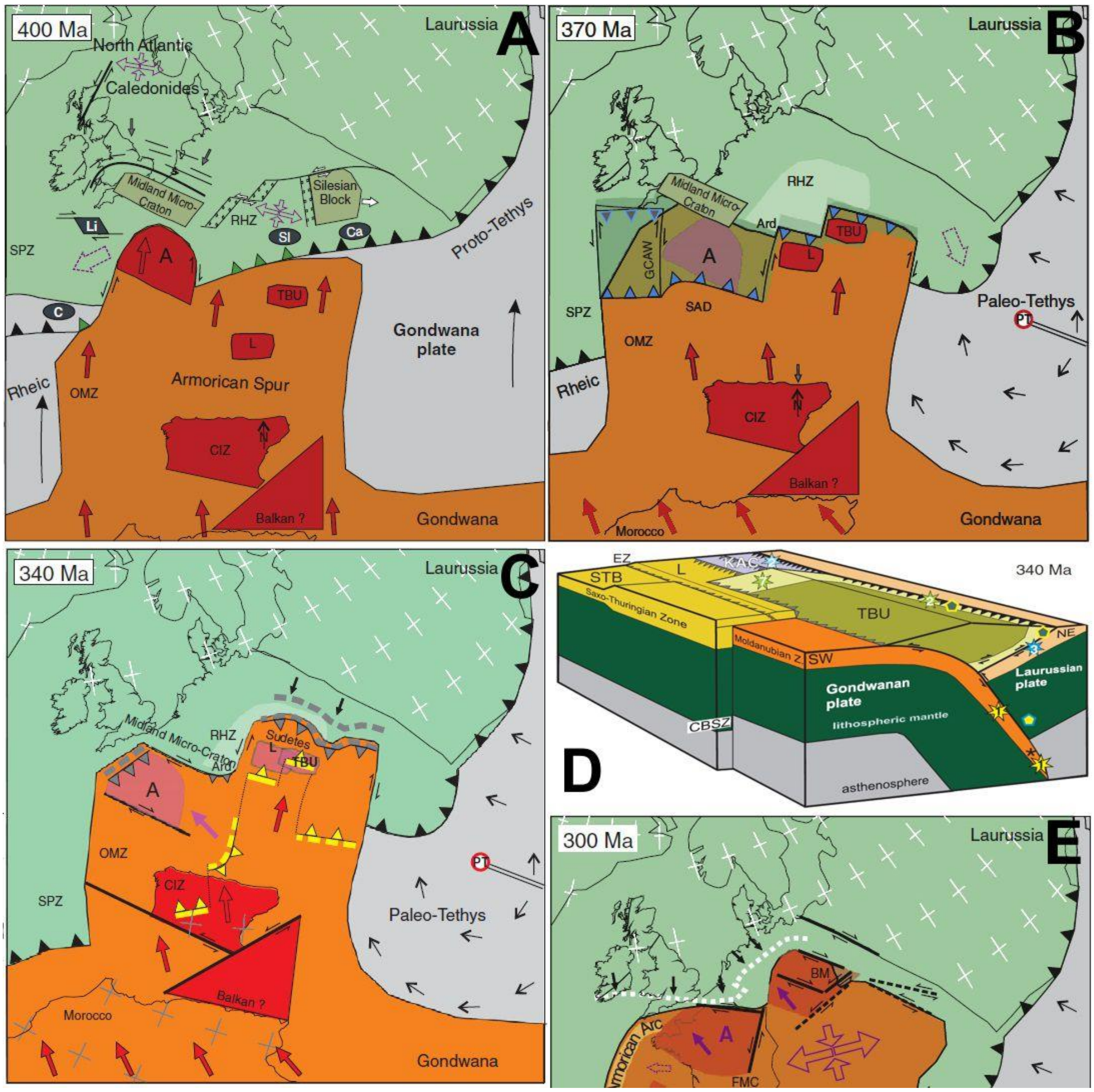

Figure 3-1. Evolution of Variscan units/terranes proposed by Kröner & Romer (2013): Li, C, Sl, Ca = Recognized ophiolites in the upper (Laurussian) plate representing trans-tensional and back-arc basins at around 400 Ma, A = Armorica, TBU = Teplá-Barrandian unit, L = Lusatia, CIZ = Central Iberian Zone, OMZ = Ossa Morena Zone, RHZ = Rheno-Hercynian Zone, GCAW = Galicia-Cornwall Accfetionary Wedge, Ard = Ardennes, SPZ = South Portuguese Zone, FMC = French Massif Central, BM = Bohemian Massif, PT = Euler Pole in the Paleotethys Ocean.

Kröner & Romer (2013) suggest that three separate subduction systems were developed during the accretion of smaller (Cadomian) terranes belonging to the Variscan orogeny: (1) Subduction zone I (410–380 Ma) with main subduction system dipping towards the north and being responsible for the initial accretion of the Armorican terrane with Laurussia (Fig. 3-1A). (2) Subduction zone II (380–360 Ma) when the main subduction jumps outwards to subduct southwards underneath the Teplá Barandien Unit (TBU; Fig. 3-1B). (3) Final subduction zone III (360–340 Ma) when another subduction developed on the SW margin of the TBU dipping towards the NE (Fig. 3-1C, D). This subduction zone was situated SW from the TBU with a transition to collision with the Moldanubian unit (MDU) at around 340 Ma, which is also the age of peak metamorphism in the SU (Kröner et al., 2007). After that, the post-orogenic development was related mainly to a dextral shearing (Fig. 3-1E).

This model, however, does not explain: (1) why sedimentary units since Upper Famenian (360 Ma) are horizontal and lie discordantly on the older Devonian sequence, as structurally and paleontologically documented in the Nepasice borehole near Hradec Králové (Čech et al., 1989; Chlupáč & Zikmundová, 1976), which implies that collision was already over at that time; (2) Subduction system III does not explain well the origin of the Central Bohemian Plutonic Complex, which was emplaced during ~354–337 Ma and has distinctive continental arc geochemistry (early calc-alkaline plutons and late ultrapotassic series; Žák et al., 2005), as the distance of plutons from the interpreted subduction zone trench (Fig. 3-2D) would extend from 20-100 km, which would require an extremely steep dipping slab or unreasonable amount of tectonic shortening. Moreover, the prolongation of the pluton is perpendicular to the MDU-TBU boundary.

Unlike Kröner & Romer (2013), Žák et al. (2014) consider that collision between STU and TBU occurred earlier, between ~380–346 Ma, along a south-dipping subduction zone (i.e., STU subducted beneath TBU at its NW margin) responsible for calc-alkaline plutons in the TBU and high-pressure metamorphism in the Erzgebirge (STU). Then, another WNW dipping subduction was responsible for the emplacements of ultrapotassic plutons in Bohemian Massif at around ~346–335 Ma. All this was followed by an overall dextral-tectonics regime between 335–315 Ma (Fig. 3-2).

Furthermore, none of the above models sufficiently explain the apparent oroclinal termination of the Variscan, with the STU apparently wrapping around the TBU and MDU in the east (Franke and Zelazniewicz, 2000). The rapid transition to post 340 Ma extension and subsequent dextral strike-slip on NW trending structures (e.g., the Elbe shear zone) are also poorly explained (e.g., Franke et al., 2014).

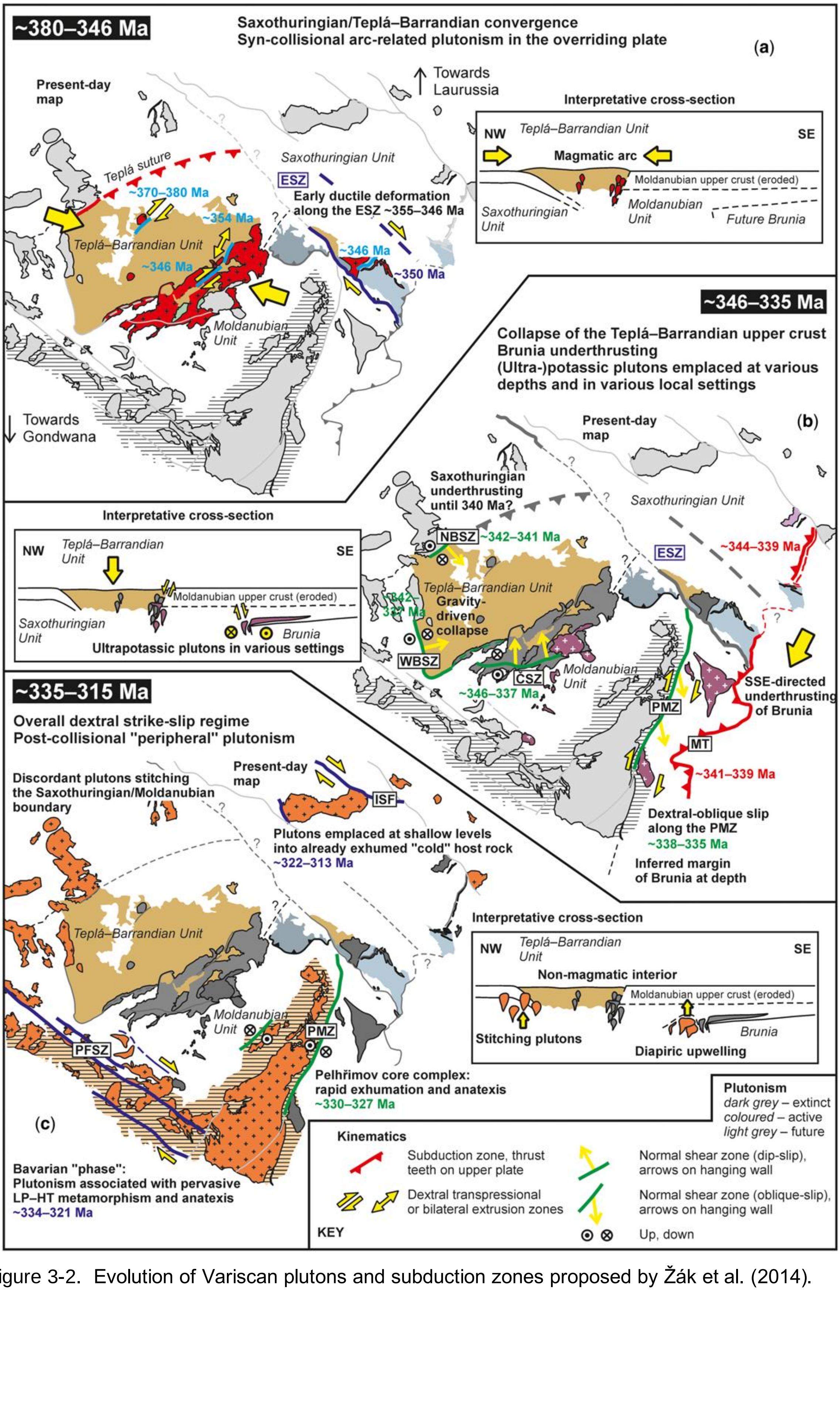

Figure 3-2. Evolution of Variscan plutons and subduction zones proposed by Žák et al. (2014).

Schulmann et al. (2014) suggest subduction of the TBU beneath STU quickly followed by a collision and exhumation of the lower crust. Unlike Kröner, he explains the Saxothuringian unit presence SE from TBU (See yellow and green areas representing STU in Fig. 3-3A) as exhumated lower crust (Figs. 3-3B-D). However, STU is affected by a lower grade of regional metamorphism than the MDU, which contradicts its interpreted lower-crustal source. Field observations also show that the STU lies structurally above the MDU, which we suggest makes their model is physically unrealistic as: (1) The suggested plastic behavior of the SU would require significant metamorphism to penetrate through the hard solid core of the MDU. However, STU outcropping inside MDU consist of shists, phyllites, marbles, cherts, quartzites, and lenses of amphibolites (i.e., low to medium grade metamorphism); (2) The STU is in general denser than the MDU, precluding standard models of lower crustal exhumation through buoyant doming.

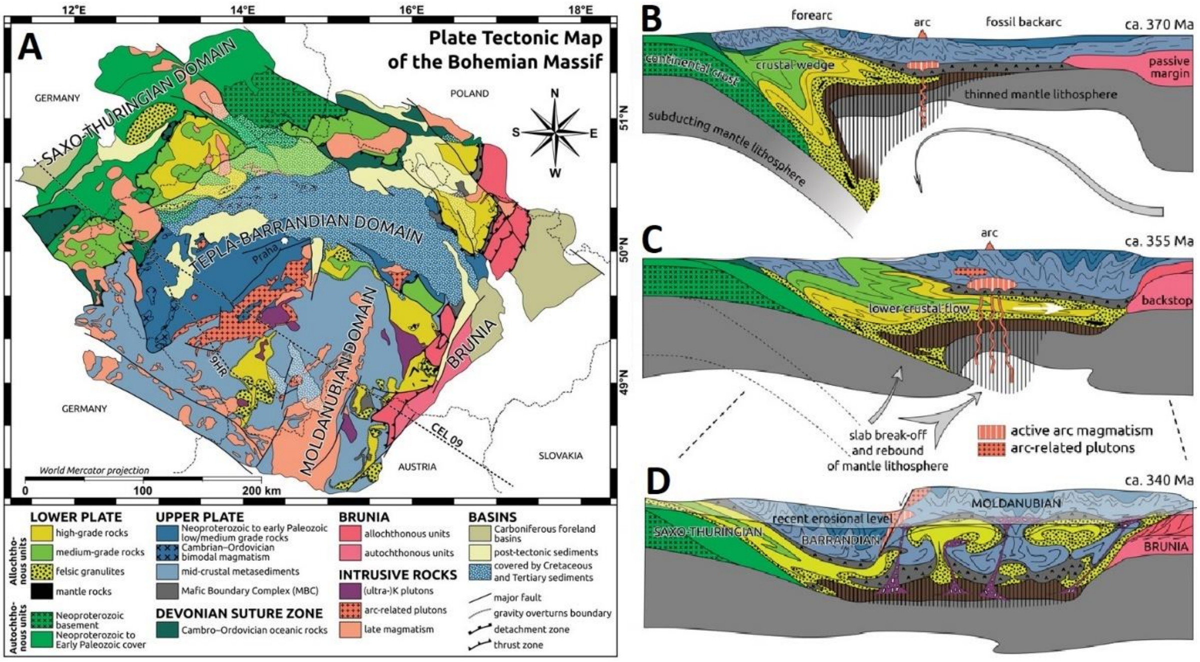

Figure 3-3. Evolution of Variscan orogen and subduction zone proposed by Schulmann et al. (2014).

Mazur et al. (2020) suggested that the main subduction zone lies far to the north, buried beneath the sedimentary cover in NE Germany between Avalonia terrain and Composite of Armorican Terranes, with a major post-collisional deformation from dextral strike-slips due to oroclinal folding of the eastern termination of the European Variscides (Fig. 3-4A). Unfortunately, their models do not give a mechanism for this oroclinal bending, nor do they precisely state the timing and, thus, does not relate the main calc-alkaline magmatic activity in Bohemian Massive (BM) to the Variscan subduction zone. However, like the other authors, they note the importance of dextral tectonic in the BM.

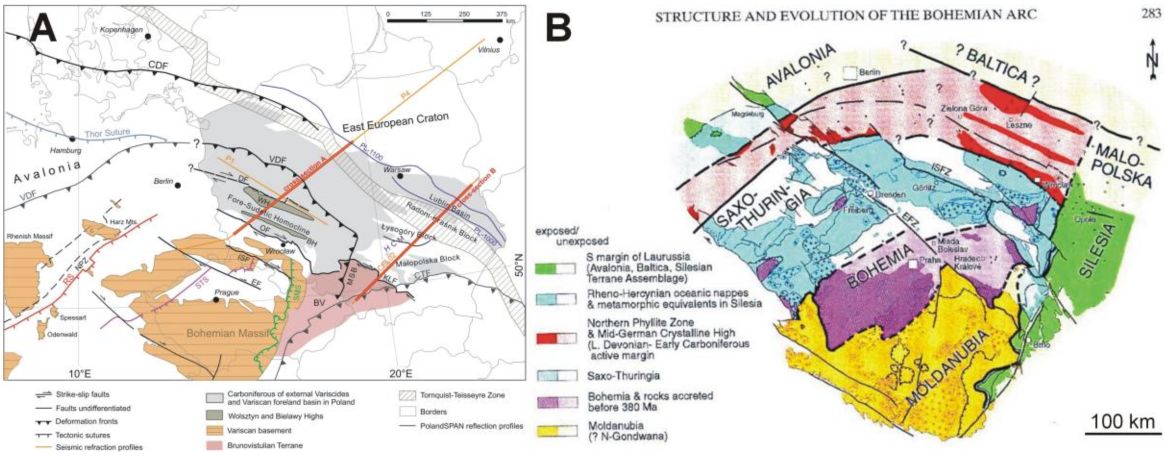

Figure 3-4. (A) Evolution of Variscan orogen and final deformation zone geometry proposed by Mazur et al. (2020): CDF = Caledonian deformation front, VDF = Variscan deformation front, CTF = Carpathian (Alpine) thrust front, RS = Rhenohercynian suture, STS = Saxothuringian suture, SMS = Staré Město suture (= Moldanubian thrust). (B) Variscan orogen architecture proposed by Franke & Zelazniwicz (2002): EFZ = Elbe fault zone, ISFZ = Intra-Sudetic fault zone.

Similarly, Franke & Zelazniwicz (2000, 2002) emphasize the significant role of the dextral transpression, without the intention of interpreting subduction zones. Unlike the other interpretations, their view is more descriptive (Fig. 3-4B), identifying, for example, at least two Permo-Carboniferous pull-apart basins in Poland. Note that these interpretations, which place a main suture zone well north of the Erzgebirge need not be incompatible with the microplate tectonics discussed by Kröner et al. (2007) and others.

While pre-Variscan and Variscan subduction zones differs in all models mentioned above, and none of them fits all the observed field data, all authors agree on the importance of post-Variscan (i.e., post-collisional) dextral strike-slip tectonics. The onset of this dextral shearing differs between the models however, which potentially has important implications for the mineral systems in the eastern Erzgebirge.

Significantly, all of these models focus mainly on explaining the accretionary phase of the Variscan orogen; while none sufficiently explain the post-peak exhumation, significant dextral strike-slip and (potential) orocline formation. In the context of this project, it is these late to post-variscan processes that are most relevant, and will be investigated in more detail. That said, the subduction zone architecture and accretionary processes that formed the Bohemian massif need to be considered by any mineral systems model, as these likely set up the architecture, fluid-pathways and potentially metallogenic fertility of the broader Erzgebirge region. Other post-orogenic processes, such as delamination or slab-breakoff, would also have significant implications for the Erzgebirge mineral system, though are generally discussed only in vague terms in the existing literature.

Finally, we note that all of the tectonic interpretations described above are based largely on geological mapping and other surface observations, resulting in significant uncertainty beneath recent sedimentary basins (e.g., the central European basin). While various geophysical data sets are available to provide key additional constraints on the crustal (and lithospheric) architecture of the Bohemian massif, we suggest that this has largely been under-utilized.

3.1.2. Data compilation

A variety of published or otherwise publicly available geological, geophysical, geochronological and mineral occurrence data have been compiled into a GIS data package as a basis for synthesis and interpretation. This has been complemented by preliminary geophysical results from the LfULG, which are proving very useful. Key datasets that are included:

- Mapped surface geology from Czech and German agencies
- Gravity + magnetic data
- Crustal seismic-reflection surveys
- Regional scale seismic tomography
- Mineralized vein occurrences and orientations
- Radiometric sampling sites with ages
- Interpreted and mapped faults
- Gamma ray spectrometry maps
- Georeferenced figures from publications (e.g., the figures in Section 3.1.1, , published ages, etc.)

We are in the process of applying a variety of standard processing techniques to the available geophysical data (e.g., upward continuations, vertical derivatives, tilt derivatives) to enhance potential subtle features. Of key interest will be the signatures of potentially ore-related structures, including (1) crustal scale boundaries such as the Elbe shear zone, pull-apart basins and tectonic terranes, and (2) local-scale structures such as intrusions, metamorphic aureole’s, and faults that potentially relate to ore deposits.

At the conclusion of the project, a series of thematic maps, cross-sections and interpretations derived from this dataset will be prepared for submission to LfULG, visualized in a way that best communicates our main findings.

3.1.3. Synthesis and preliminary interpretations

So far, our efforts have focused on understanding the post-peak metamorphism Variscan transtensional structures, such as the Elbe Shear Zone (ESZ), and their links to magmatism and associated mineralization. The ESZ is a major geological structure that forms the prominent eastern border of the Erzgebirge, separating the well-endowed Erzgebirge from the Lausitz Block, which contains only scant magmatic-hydrothermal mineralization.

The ESZ is well known to be a long-lived (and still ongoing) tectonic structure, with mostly dextral kinematics and a total (interpreted) offset of ~40–50 km. It has been subject to a complex interplay of late to post-Variscan tectonic, magmatic, and sedimentary processes, which have left a distinct signature in the magmatic and sedimentary rock record. At least two distinct transtensional events can be distinguished and attributed to the dextral activity on the ESZ. These are recorded by (1) the Meissen Massif, a complex intrusion that was emplaced at 330–320 Ma (Sharp et al., 1997; Nasdala et al., 1999) in a dilatational jog (Kröner et al., 2007), and (2) the Döhlen Basin near Freital, the volcano-sedimentary infill of a small pull-apart basin with abundant ignimbrite/tuff units ranging in age from ~294–286 Ma. The latter evidence for a tectonic reactivation along the ESZ and synchronous magmatic events (Zieger et al., 2019).

These ages bracket a potentially extensive period of activity of the ESZ, supporting the potential for a spatio-temporal link between the ESZ and formation of the Tharandt and Altenberg-Teplice Calderas at ~315–310 Ma (Tomek et al., 2021). The latter is well known to host a number of small granitic stocks with related Sn-Li/W-(Mo) mineralization. Significantly, these zones of strain-transfer between NW–SE trending dextral strike-slip faults localize felsic magmatism, by accommodating intrusions and establishing favorable pathways to the lower crust through which melts can ascend. This interpretation is supported by the generally A-type granite composition of mineralized intrusions (Klomínský et al., 2010), which commonly occur along shear zones during within-plate transtension (e.g., Collins et al., 2019).

Recognized epithermal veins and greisen-type Sn, and W mineralization in the Eastern Erzgebirge are mostly of Paleozoic age and, with better geochronology, can likely be linked with specific tectonic and/or magmatic events. Precise dating of intra- and extra- ATC caldera rhyolites and ring dykes (Tomek et al., 2021; Tichomirowa et al., 2022; Casas-Garcia et al., 2019) allows direct linking to Sn deposits of the same age (Seifert et al., 2011; Leopardi et al., *submitted*). The role of contemporaneous dextral wrenching tectonics in the Bohemian Massif (Edel et al., 2021; Bárta et al., 2021) remains unclear, but we suggest likely structural controls the localization of pluton emplacement and their accommodation and growth. An analogous situation can be observed in the western Erzgebirge (albeit likely at a deeper crustal level), where granitic plutonism and associated Sn and W mineralization is clearly associated with major NW trending dextral strike-slip structures (Fig. 3-5).

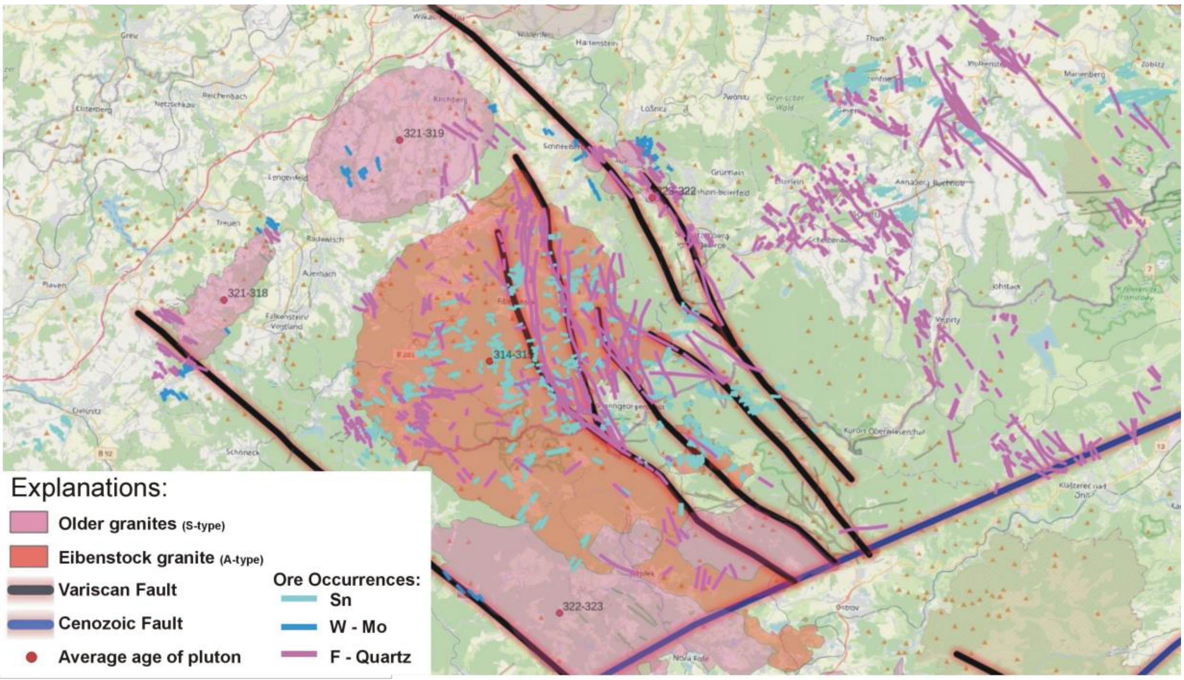

Figure 3-5. Tectonic situation on the eastern margin of the Eibenstock pluton and related ore deposits. Plutons clearly sit within a transtensional jog (and possible flower structure) within the broader Gera-Jáchymov fault system. Significantly, this fault system appears to also control the major overprinting mineralized F-Quartz vein systems.

It is likely that the same tectonic regime applied also to the Eastern Erzgebirge, which is supported by previously provided references and summarized in the tectonostratigraphic chart for the Paleozoic Era for the Erzgebirge region (Fig. 3-6). The similar age of the Eibenstock pluton and Altenberg-Teplice caldera (ATC) strongly suggests that magmatic system beneath the caldera was emplaced in the same setting, and potentially that similar fault systems can be expected at depth. Comparison of the Western and Eastern Erzgebirge (and considering their different erosional level) reveals two additional potential analogies: (1) one might expect significant fluorite vein deposits along emplacement-related faults beneath the ATC, as in the Western Erzgebirge, and; (2) W-Mo mineralization could be associated with relatively older intrusions crosscut by Sn-rich ones at ~315 Ma, as is observed at Eibenstock (Fig. 3-5 and 3-7).

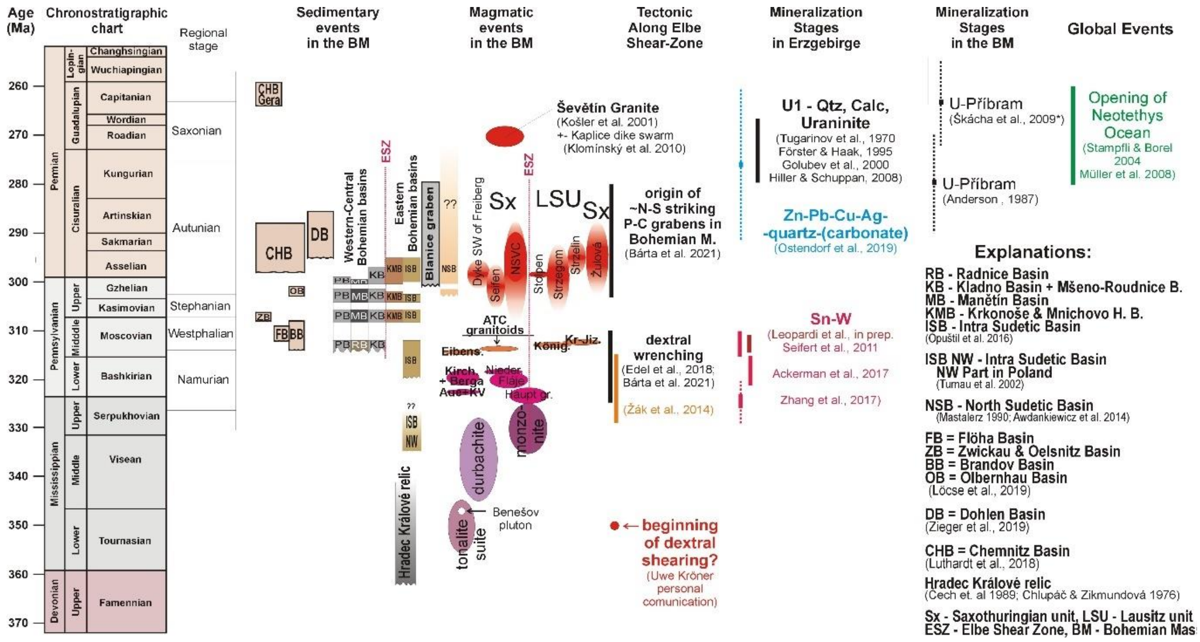

Figure 3-6. Tectonostratigraphic chart with ages of ore deposits for the Paleozoic Era in the BM. The compiled chart is based on following references: Tectonic events – Bárta et al. (2021), Edel et al. (2018), Žák et al. (2014); Magmatic events – Bárta et al. (2021), Breitkreuz et al. (2021), Casas-García et al. (2019) Förster & Rhede (2006), Hoffmann et al. (2009, 2013), Löcse et al. (2019), Kässner et al. (2021), Klomínksý et al. (2010), Košler et al. (2001), Kryza et al. (2014), Laurent et al. (2014), Nasdala et al. (1999), Oberc-Dziedzic & Kryza (2012), Sharp et al. (1997), Tichomirowa et al. (2019, 2022), Tomek et al. (2021), Turniak et al. (2014), Wenzel et al. (1997); Mineralization events – Ackerman et al. (2017), Anderson (1987), Förster & Haak (1995), Golubev et al. (2000), Hiller & Schuppan (2008), Ostendorf et al. (2019), Seifert et al. (2011), Škácha et al. (2009), Tugarinov et al. (1970), Zhang et al. (2017); Sedimentary events – Awdankiewicz et al. (2014), Chlupáč & Zikmundová (1976), Čech et al. (1989), Löcse et al. (2019), Luthardt et al. (2018), Mastalerz (1990), Opuštil et al. (2016), Turnau et al. (2002), Zieger et al. (2019); Global events – Stampfli & Borel (2004), Müller et al. (2008).

Known W-Mo mineralization around relatively older Telnice granite and northern part of the Fláje pluton in the Eastern Erzgebirge have been reported (Uwe Lehmann, personal communication), while Sn mineralization is well known around intrusions (312-314 Ma, and possibly ~301 ±5 Ma near Seiffen; Th-U-Pb on monazite & K-Ar on Siderophyllite, Förster & Rhede 2006). Fluorite-quartz veins are also reported from Sadisdorf (Dino Leopardi, personal communication), although their timing is unclear. Lastly, our analogy to the Western Erzgebirge would imply that published ages for the Markersbach (ICP-MS; 327 ±4 Ma; Hofmann et al., 2009) and most likely also the Telnice granite (K-Ar; 338 Ma; Štemprok et al., 2003) are likely incorrect, because the Markersbach granite penetrates the Elbe shear zone and, therefore, it should be one of the youngest intrusions in the area (certainly younger than the Meissen Massif). Moreover, associated Sn mineralization occurrences around Markersbach suggest that this pluton should be of similar age as the ATC granites. The only available radiometric age for the Telnice granite ages is in literature referred to as "personal communication" with no actual data provided (Štemprok et al., 2003). The age is thus deemed unreliable and likely too old, as this would make it the oldest plutonic body in the Eastern

Erzgebirge – essentially coinciding with the age of peak Variscan metamorphism. Furthermore, it would be of the same age as the Central Bohemian Plutonic Complex. Moreover, the fact that W-Mo mineralization is related to the Telnice granite may be used to suggest that this granite is at least 20 Ma younger than the currently available age.

From, it is suggested to obtain new radiometric ages for the Markersbach granite, the Telnice granite – as well as the currently undated Schellerhau granite in order to provide a more consistent magmatic and geotectonic Framework for the Eastern Erzgebirge and its magmatic-hydrothermal mineral systems.

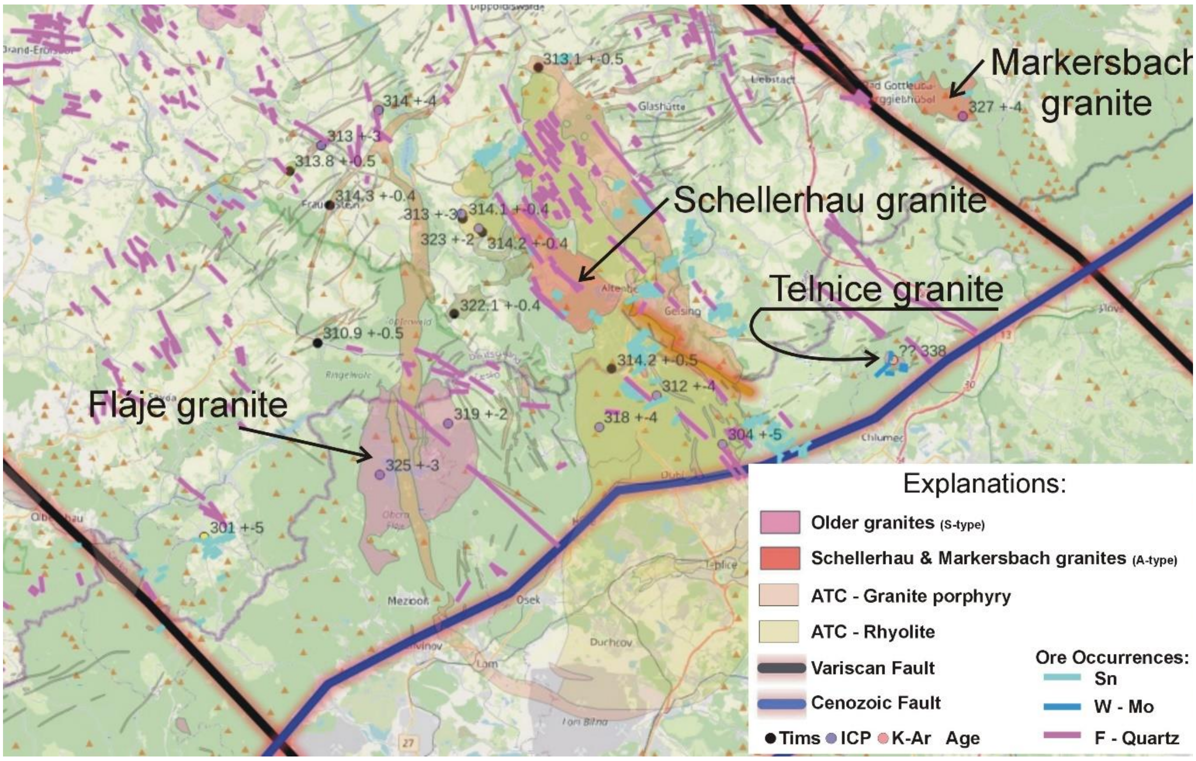

Figure 3-7. Tectonic situation on the Eastern Erzgebirge study region and related magmatic-hydrothermal ore deposits.

3.3. Next steps

At the current stage, structural data from historic maps and other publications (Baumann, Hofmann, etc.) are still being collated for the magmatic and epithermal systems in the eastern Erzgebirge. Once complete, these will provide the foundation for a structural analysis of the fluid pathways that controlled mineralization, and potentially the broader stress regime during mineralization.

Newly provided magnetic and gravity data are being analyzed and (re)-processed (e.g., high-pass filtering, gradients) to allow a joint geology and geophysical interpretation of the eastern Erzgebirge. These will provide a basis to better evaluate published tectonic models for the region and the link between tectonics and mineralization.

4. WP 3 to 5 - Mineral Systems Analysis

These work packages will be the focus of future reports, once more progress has been made in WP-2 and WP-3.

However, to help place our preliminary work in context, we have included a brief conceptual model for the Eastern Erzgebirge mineral system (Fig. 4-1). This will evolve significantly over the course of this project, but hopefully serves as a useful starting point for discussions. It highlights key elements that likely control the epithermal and magmatic mineral systems, and the (potential) commonalities between them. While a detailed review of the literature on the metallogenesis of the Freiberg district is out-of-scope for this progress report, the many question marks in the diagram emphasize that significant uncertainty exists.

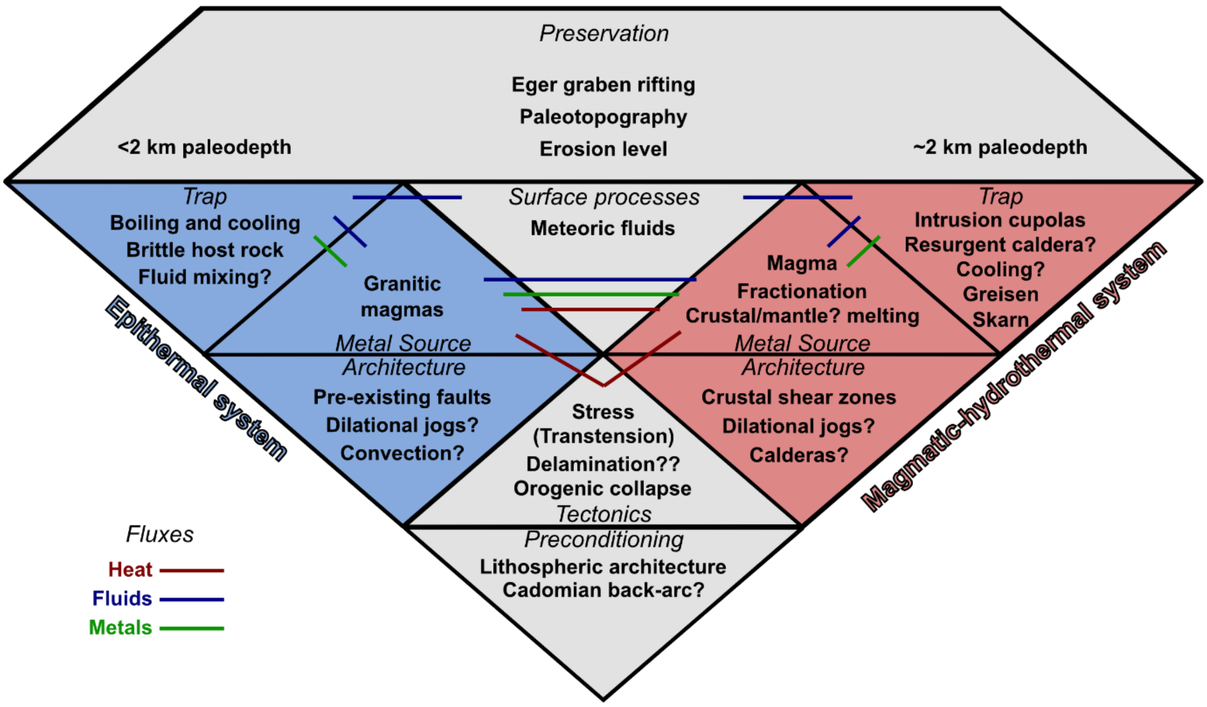

Figure 4-1. Summary diagram highlighting the key components and fluxes that are likely to play a role in the Eastern Erzgebirge mineral systems. Common elements are shown in grey, epithermal-specific processes in blue and magmatic-specific processes in red. The main fluxes are also schematically overlain as colored arrows.

This conceptual model has allowed us to develop several working hypotheses for the Paleozoic mineral systems in the Erzgebirge:

1. Sn-Li-W-Mo deposits can be divided into two subtypes: (1) Sn-Li-dominated and (2) W-Mo-dominated deposits. Both these subtypes are clearly directly linked with magmatic systems. The Sn-Li-dominated deposits occur in greisens, greisenised lenses, veins, and stockworks, while the W-Mo-dominated mineralization is almost solely related to quartz veins and stockworks (e.g., Štemprok & Blecha, 2015). The geographical distribution of Sn-Li and W-Mo dominated deposits differ, suggesting either different mobility, or association with magmatism of different ages (312–315 Ma vs. 318–322 Ma). Nevertheless, the Sadisdorf deposit contains not only Sn and Li, but also Mo. This may be explained by a higher susceptibility of Mo for remobilization due to thermo-chemical sulfate reduction (i.e., 80 < T < 200 °C; Ardakani et al., 2016).

2. Epithermal Pb-Zn-Ag: Although often inferred, a magmatic system that can be directly related to this/these deposits remains unknown. Fluid inclusion analyses has shown that fluids are partly of magmatic origin and partly of hydrothermal origin (Burisch et al., 2019b; Bauer et al., 2019; Swinkels et al., 2021), as is typical in epithermal systems. Various factors likely control the emplacement of these deposits, including:
    1. A suitable host rock to facilitate brittle vein formation
    2. Pre-existing structures oriented favorably for fluid flow relative to the stress field (e.g., dilational jogs)
    3. Vicinity of a suitable parental magmatic system. Magmatic rocks possibly related to such magmatic system and their ages are listed in the supplementary table (Appendix 1)
    4. Suitable source rocks which might have fertilized magma
    5. Depth below the paleosurface and preservation potential due to subsequent uplift and erosion

So far, it is unclear which of these factors played the most significant role in the eastern Erzgebirge, nor how they can be used to predict undiscovered mineralization. Nevertheless, we can speculate that the mineralized veins originated during (1) trans-tensional or (2) extensional regimes following the collapse or dismemberment of the Variscan orogen. Further analyses will be focused on resolving these essential questions.

5. WP 6 - Publication and dissemination

Two abstracts covering the preliminary results of work packages 1 and 2 have been submitted for the 10th Hutton Symposium on granites and related rocks (10-15 September 2023 in Italy; https://hutton10.eu/). As we are in the early stage of the "Neues Potential" project, nothing has been decided yet concerning publication in peer-reviewed international journals, however this is expected over the next ~1 year.

6. References

Ackerman L., Haluzová E., Creaser R. A., Pašava J., Veselovský F., Breiter K., Erban V. & Drábek M. (2017). Temporal evolution of mineralization events in the Bohemian Massif inferred from the Re–Os geochronology of molybdenite. Mineralium Deposita, vol. 52(5), 651–662. https://doi.org/10.1007/s00126-016-0685-5

Anderson E.B. (1987). Isotopic-Geochronological Investigation of the Uranium Mineralization of Czechoslovakia; MS DIAMO: Příbram, Czech Republic.

Ardakani O.H., Chappaz A., Sanei H. & Mayer B. (2016). Effect of thermal maturity on remobilization of molybdenum in black shales. Earth Planet. Sci. Lett. Vol. 449, 311-320.

Atanasova P. (2012). Mineralogy, geochemistry and age of greisen mineralization in the Li-Sn(-W) deposit Zinnwald, Eastern Erzgebirge, Germany. Master thesis, TU Bergakademie Freiberg. 93p.

Awdankiewicz M., Kryza R. & Szczepara N. (2014). Timing of post-collisional volcanism in the eastern part of the Variscan Belt: Constraints from SHRIMP zircon dating of Permian rhyolites in the North-Sudetic Basin (SW Poland). Geological Magazine, vol. 151(4), 611-628. Doi:10.1017/S0016756813000678

Bauer M.E., Burisch M., Ostendorf J., Krause J., Frenzel M., Seifert T. & Gutzmer J. (2019) Trace element geochemistry of sphalerite in contrasting hydrothermal fluid systems of the Freiberg district, Germany: insights from LA-ICP-MS analysis, near-infrared light microthermometry of sphalerite-hosted fluid inclusions, and sulfur isotope geochemistry. Miner Deposita vol. 54, 237-262. https://doi.org/10.1007/s00126-018-0850-0

Baumann L. (1965). Die Erzlagerstätten der Freiberger Randgebiete. Thesis, TU Bergakademie Freiberg

Bárta O., Melichar R. & Černý J. (2021). How many extensional stages marked the Variscan gravitational collapse in the Bohemian Massif? Ann Soc Geol Pol vol. 91(2),121-136.

Burisch M., Gerdes A., Walter B. F., Neumann U., Fettel M. & Markl G. (2017). Methane and the origin of five-element veins: mineralogy, age, fluid inclusion chemistry and ore forming processes in the Odenwald, SW Germany: Ore Geology Reviews, v. 81, 42-61.

Burisch M., Gerdes A., Meinert L. D., Albert R., Seifert T. & Gutzmer J. (2019a). The essence of time – fertile skarn formation in the Variscan Orogenic Belt: Earth and Planetary Science Letters, v. 519, 165-170. https://doi.org/10.1016/j.epsl.2019.05.015

Burisch M., Hartmann A., Bach W., Krolop P., Krause J. & Gutzmer J. (2019b) Genesis of hydrothermal silver-antimony-sulfide veins of the Bräunsdorf sector as part of the classic Freiberg silver mining district, Germany. Miner Deposita vol. 54, 263-280. https://doi.org/10.1007/s00126-018-0842-0

Breiter K. (2008). Mineral and textural evolution of subvolcanic A-type granite: Hora Svat Kateriny stock, Krusne Hory Mts., Czech Republic. Z. f. geol. Wiss. vol. 36, issue 6, 365-382.

Breitkreuz C., Lapp M., Käßner A., Tichomirowa M., Lapp M., Huang S. & Stanek K. (2021). The Late Carboniferous deeply eroded Tharandt Forest Caldera-Niederbobritzsch Granite Complex: A post-

Variscan long-standing magmatic system in central Europe. Int J Earth Sci 110,1265-1292. https:// doi. org/ 10. 1007/ s00531- 021- 02015-x

Casas-García R., Rapprich V., Breitkreuz C., Svojtka M., Lapp M., Stanek K., Hofmann U. & Linnemann U. (2019). Lithofacies architecture, composition, and age of the Carboniferous Teplice Rhyolite (German-Czech border): Insights into the evolution of the Altenberg-Teplice Caldera, Journal of Volcanology and Geothermal Research, vol. 386, 106662. doi:10.1016/j.jvolgeores.2019.106662

Chlupáč I. & Zikmundová J. (1976). The Devonian and Lower Carboniferous in the Nepasice bore in East Bohemia. Věstník Ústředního Ústavu Geologického, vol. 51, 269-278. Praha.

Collins W.J., Huang H.-Q., Bowden P. & Kemp A.I.S. (2019). Repeated S- I- A-type granite trilogy in the Lachlan Orogen, and geochemical contrasts with A-type granites in Nigeria: Implications for petrogenesis and tectonic discrimination. (*In*) Janoušek V., Bonin B., Collins W.J., Farina F. & Bowden P. (*eds*): Post-Archean Granitic Rocks: Petrogenetic Processes and Tectonic Environments. Geological Society, London, Special Publications 491.

Cymerman Z. (2000). Paleozoic Orogeneses in the Sudetes: a Geodynamic Model. Geological Quarterly vol. 44, 59-80.

Čech S., Havlíček V. & Zikmundová J. (1989). The Upper Devonian and Lower Carboniferous in north-eastern Bohemia (based on boreholes in the Hradec Králové area). Věstník Ústředního Ústavu Geologického, vol. 64, 65-70. Praha.

Dolejš D.& Štemprok M. (2001). Magmatic and hydrothermal evolution of Li-F granites: Cínovec and Krásno intrusions, Krušné hory batholith, Bull. Czech Geol. Survey, vol. 76, 77-99.

Edel J. B., Schulmann K., Lexa O. & Lardeaux J. M. (2018). Late Palaeozoic palaeomagnetic and tectonic constraints for amalgamation of Pangea supercontinent in the European Variscan belt. Earth-Science Reviews, vol. 177, 589-612.

Förster B. & Haack U. (1995). U/Pb-Datierungen von Pechblenden und die hydrothermale Entwicklung der U-Lagerstätte Aue-Niederschlema (Erzgebirge). Zeitschrift für Geologische Wissenschaften, vol. 23 (5/6), 581-588.

Förster H.-J., Tischendorf G., Seltmann R. & Gottesmann B. (1998). Die variszischen Granite des Erzgebirges: neue Aspekte aus stofflicher Sicht. Z geol Wiss, vol. 26, 31-60.

Förster H.-J. & Rhede D. (2006). The Be–Ta-rich granite of Seiffen (eastern Erzgebirge, Germany): Accessory-mineral chemistry, composition and age of a late-Variscan Li–F granite of A-type affinity. N. J. Miner. Abh., vol. 182, 307-321.

Förster H.-J., Gottesmann B., Tischendorf G., Siebel W., Rhede D., Seltmann R. & Wasternack J. (2007). Permo-Carboniferous subvolcanic rhyolitic dikes in the western Erzgebirge/Vogtland, Germany. A record of source heterogeneity of post-collisional felsic magmatism. Neues Jahrbuch für Mineralogie-Abhandlungen: Journal of Mineralogy and Geochemistry, vol. 183(2), 123-147.

Franke W. (2014). Topography of the Variscan orogen in Europe: failed – not collapsed. Int. J. Earth Sci. Geol. Rundsch. vol. 103, 1471-1499.

Franke W. & Żelaźniewicz A. (2000). The eastern termination of the Variscides: terrane correlation and kinematic evolution. (*In*) Franke, W., Haak, V., Oncken, O., Tanner, D. (*ds.*), Orogenic Processes: Quantification and Modelling in the Variscan Belt. Geological Society, London, Special Publications, vol. 179, 63-86. https://doi.org/10.1144/GSL.SP.2000.179.01.06.

Franke W. & Żelaźniewicz A. (2002). Structure and evolution of the Bohemian Arc. (*In*) Winchester JA, Pharaoh TC, Verniers J (*eds*) Palaeozoic Amalgamation of Central Europe, Geological Society, Special Publications, London, vol. 201, 279-293. https://doi.org/10.1144/GSL.SP.2002.201.01.13

Gerstenberger H. (1989). Autometasomatic Rb enrichments in highly evolved granites causing lowered Rb-Sr isochron intercepts. Earth and Planetary Science Letters vol. 93(1), 65-75.

Golubev V. N. Cuney M. & Poty, B. (2000). Phase composition and U-Pb pitchblende systems of quartz-calcite-pitchblende veins at the Schlema-Alberoda deposit (Erzgebirge): Geology of Ore Deposits, vol.42, 513-525.

Guilcher M., Albert R., Gerdes A., Gutzmer J. & Burisch M. (2021). Timing of native metal-arsenide (Ag-Bi-Co-Ni-As±U) veins in continental rift zones – in situ U-Pb geochronology of carbonates from the Erzgebirge/Krušné Hory province. Chemical Geology, vol. 584, 120476.

Haack U. (1990). Datierung mit Rb/Sr Mischungslinien? Berichte der Deutschen Mineralogischen Gesellschaft, Beihefte Zum European Journal of Mineralogy, vol. 2, 1-86.

Hiller A. & Schuppan W. (2008). Geologie und Uranbergbau im Revier Schlema-Alberoda, first edition ed. Sächsisches Landesamt für Umwelt und Geologie (LfUG), Germany, 171p.

Hoffmann U., Breitkreuz C., Breiter K., Sergeev S., Stanek K. & Tichomirowa M. (2013). Carboniferous—Permian volcanic evolution in Central Europe—U/Pb ages of volcanic rocks in Saxony (Germany) and northern Bohemia (Czech Republic). Int J Earth Sci vol. 102(1), 73-99.

Hofmann M., Linnemann U., Gerdes A., Ullrich B. & Schauer M. (2009). Timing of dextral strike-slip processes and basement exhumation in the Elbe Zone (Saxo-Thuringian Zone): the final pulse of the Variscan orogeny in the Bohemian Massif constrained by LA-SF-ICP-MS U-Pb zircon data. Geol Soc London Spec Publ vol. 327, 197-214.

Höhndorf A., Kämpf H. & Dulski P. (1994). Sm/Nd and Rb/Sr isotopic investigations on fluorite mineralization of the eastern Erzgebirge. (*In*) Seltmann, R., Kämpf, H., Möller, P. (*eds*) Metallogeny of collisional orogens. Czech Geological Survey, Praha, 116-128.

Hoth K., Tischendorf G., Berger H. J., & et al. (1980). Geologische Karte Erzgebirge/Vogtland.: Dresden, Sächsisches Landesamt für Umwelt, Landwirtschaft und Geologie.

Käßner A., Tichomirowa M., Lapp M., Leonhardt D., Whitehouse M. & Gerdes A. (2021). Two-phase late Paleozoic magmatism (~ 313–312 and ~ 299–298 Ma) in the Lusatian Block and its relation to large scale NW striking fault zones: evidence from zircon U–Pb CA–ID–TIMS geochronology, bulk rock- and zircon chemistry. Int J Earth Sci (Geol Rundsch), vol. 110, 2923-2953. https://doi.org/10.1007/s00531-021-02092-y

Kempe U. & Belyatsky B. V. (1997). An attempt at direct dating of the Sadisdorf Sn-W mineralization, Eastern Erzgebirge (Germany). Journal of the Czech Geological Society, vol. 42(3), 21.

Kempe U., Wolf D., Ebermann U. & Bombacj K. (1999). 330 Ma Pb/Pb single zircon evaporation ages for the Altenberg granite porphyry, Eastern Erzgebirge (Germany): implication for Hercynian granite magmatism and tin mineralization. Z. geol. Wiss. vol. 27(5/6), 385-400.

Kempe, U. (2003). Precise electron microprobe age determination in altered uraninite: consequences on the intrusion age and the metalloenic significance of the Kirchberg granite (Erzgebirge, Germany). Contributions to Mineralogy and Petrology vol. 145(1), 107-118.

Kempe U., Bombach K., Matukov D., Schlothauer T., Hutschenreuter J., Wolf D. & Sergeev S. (2004). Pb/Pb and U/Pb zircon dating of subvolcanic rhyolite as a time marker for Hercynian granite magmatism and Sn mineralisation in the Eibenstock granite, Erzgebirge, Germany: Considering effects of zircon alteration. Miner Deposita, vol. 39, 646-669. https://doi.org/10.1007/s00126-004-0435-y

Kiefer S., Števko M., Vojtko R., Ozdín D., Gerdes A., Creaser R. A., Szczerba M. & Majzlan J. (2020). Geochronological constraints on the carbonate-sulfarsenide veins in Dobšiná, Slovakia: U/Pb ages of hydrothermal carbonates, Re/Os age of gersdorffite, and K/Ar ages of fuchsite: Journal of the Czech Geological Society, 229–247.

Klomínský J., Jarchovský T. & Rajpoot G.S. (2010). Atlas of plutonic rocks and orthogneisses in the Bohemian Massif. Czech Geological Survey.

Košler J., Kelley S. & Vrána S. (2001). $^{40}Ar/^{39}Ar$ hornblende dating of a microgranodiorite dyke: implications for early Permian extension in the Moldanubian Zone of the Bohemian Massif. Int J Earth Sci vol. 90, 379-385. https://doi.org/10.1007/s005310000154

Kováríková P., Siebel W., Jelínek E., Štemprok M., Kachlík V., Holub F.V. & Blecha V. (2007). Petrology, geochemistry and zircon age for redwitzite at Abertamy, NW Bohemian Massif (Czech Republic): tracing the mantle component in Late Variscan intrusions. Chemie der Erde-Geochemistry vol. 67(2), 151-174.

Kroner U., Hahn T., Romer R.L. & Linnemann U. (2007). The Variscan orogeny in the Saxo-Thuringian zone—Heterogenous overprint of Cadomian/Paleozoic Peri-Gondwana crust. (*In*) Linnemann et al.

(*eds*) The evolution of the Rheic Ocean: From Avalonian-Cadomian active margin to Alleghenian-Variscan collision. Geological Society of America Special Paper 423, 153-172.

Kroner U. & Romer R.L. (2013). Two plates – Many subduction zones: The Variscan orogeny reconsidered: Gondwana Research, vol. 24, 298-329.

Laurent A., Janoušek V., Magna T., Schulman K., Míková J. (2014). Petrogenesis and geochronology of a post-orogenic calc-alkaline magmatic association: the Žulová Pluton, Bohemian Massif. J Geosci vol. 59, 415-440. https://doi.org/10.3190/jgeosci.176

Leopardi D., Gerdes A., Albert R., Gutzmer J., Lehmann B. & Burisch M. (2023). LA-ICP-MS U-Pb cassiterite age data of the Sadisdorf deposit link Sn-Li-(W-Cu) mineralization in the eastern Erzgebirge to the collapse of the Altenberg-Teplice Caldera. Manuscript submitted.

Löcse F., Linnemann U., Schneider G., Merbitz M. & Rößler R. (2019). First U–Pb LA-ICP-MS zircon ages assessed from a volcanosedimentary complex of the mid-European Variscides (Pennsylvanian, Flöha Basin, SE Germany) International Journal of Earth Sciences, vol. 108, 713-733. https://doi.org/10.1007/s00531-019-01684-z

Luthardt L., Hofmann M., Linnemann U., Gerdes A., Marko L. & Rößler R. (2018). A new U–Pb zircon age and a volcanogenic model for the early Permian Chemnitz Fossil Forest. Int J Earth Sci. vol. 107, 2465-2489. https://doi.org/10.1007/s0053 1-018-1608-8

Mastalerz K. (1990). Lacustrine Succesions in Fault-Bounded Basins: 1. Upper Anthracosia Shale (Lower Permian) of the North Sudetic Basin, SW Poland. Annales Societatis Geologorum Poloniae, vol. 60, 75-106.

Mazur S., Aleksandrowski P., Gągała Ł., Krzywiec P., Żaba J., Gaidzik K. & Sikora R. (2020). Late Palaeozoic strike-slip tectonics versus oroclinal bending at the SW outskirts of Baltica: case of the Variscan belt's eastern end in Poland. Int. J. Earth Sci. vol. 109, 1133-1160. https://doi.org/10.1007/s00531-019-01814-7

Müller A., Breiter K., Seltmann R. & Pésckay Z. (2005). Quartz and feldspar zoning in the eastern Erzgebirge volcano-plutonic complex (Germany, Czech Republic): evidence of multiple magma mixing. Lithos, vol. 80(1), 201-227.

Müller R.D., Sdrolias M., Gaina C. & Roest W.R. (2008). Age, spreading rates and spreading symmetry of the world's ocean crust, Geochem. Geophys. Geosyst., vol. 9, Q04006, doi:10.1029/2007GC001743.

Nasdala L., Wenzel T., Pidgeon R.T. & Kronz A. (1999). Internal structures and dating of complex zircons from Meissen Massif monzonites, Saxony. Chem Geol, vol. 156, 331-341.

Neßler J. (2016). Geologischer Aufbau, Mineralogie, Geochemie und Geochronologie der Li-Sn-W-Greisenlagerstätte Zinnwald, Osterzgebirge, Deutschland. PhD thesis, TU Bergakademie Freiberg, 399p.

Oberc-Dziedzic T. & Kryza R. (2012). Late stage Variscan magmatism in the Strzelin Massif (SW Poland): SHRIMP zircon ages of tonalite and Bt-Ms granite of the Gęsiniec intrusion. Geol Q, vol. 56, 225-236.

Oliver G.J.H., Corfu F., Krogh & T.E. (1993). U-Pb ages from SW Poland: evidence for a Caledonian suture zone between Baltica and Gondwana. Journal of the Geological Society, vol. 150, 355-369. https://doi.org/10.1144/gsjgs.150.2.0355

Opluštil S., Schmitz M., Cleal C. J. & Martínek K. (2016). A review of the Middle-Late Pennsylvanian west European regional substages and floral biozones, and their correlation to the Geological Time Scale based on new U-Pb ages. (*In*) Earth-Science Reviews, Elsevier. vol. 154, 301–335https://doi.org/10.1016/j.earscirev.2016.01.005

Ostendorf J., Henjes-Kunst F., Seifert T. & Gutzmer J (2019). Age and genesis of polymetallic veins in the Freiberg district, Erzgebirge, Germany: constraints from radiogenic isotopes. Miner Deposita vol. 54, 217-236.

Reinhardt N., Gerdes A., Beranoaguirre A., Frenzel M., Meinert L. D. Gutzmer, J. & Burisch M. (2022). Timing of magmatic-hydrothermal activity in the Variscan Orogenic Belt: LA-ICP-MS U–Pb geochronology of skarn-related garnet from the Schwarzenberg District, Erzgebirge: Mineralium Deposita, vol. 57, 1071-1087.

Roberts N. M. W., Drost K., Horstwood M. S. A., Condon D. J., Chew D., Drake H., Milodowski A. E., McLean N. M., Smye A. J., Walker R. J., Haslam R., Hodson K., Imber J., Beaudoin N. & Lee J. K. (2020). Laser ablation inductively coupled plasma mass spectrometry (LA-ICP-MS) U-Pb carbonate geochronology: strategies, progress, and limitations: Geochronology, vol. 2, 33-61.

Romer R. L., Thomas R., Stein H. J. & Rhede D. (2007). Dating multiply overprinted Sn-mineralized granites—examples from the Erzgebirge, Germany: Miner. Deposita, vol. 42, 337-359.

Romer R. L., Förster H.-J. & Štemprok M. (2010). Age constraints for the late-Variscan magmatism in the Altenberg–Teplice Caldera (Eastern Erzgebirge/Krušné hory): N. Jb. Miner. Abh., vol. 187, 289-305.

Seltmann R. & Schilka W. (1995). Late Variscan crustal evolution in the Altenberg–Teplice caldera. Evidence from new geochemical and geochronological data: Terra Nostra, vol. 98, 120-124.

Seifert T. (2008). Metallogeny and petrogenesis of lamprophyres in the Mid-European Variscides: Post-collisional magmatism and its relationship to ate-Variscan ore forming processes in the Erzgebirge (Bohemian Massif), IOS Press BV, Amsterdam. 303p.

Seifert T., Atanasova P., Gutzmer J. & Pfänder J. (2011). Mineralogy, geochemistry and age of greisen mineralization in the Li-RbCs-Sn-W deposit Zinnwald, Erzgebirge, Germany development View project. Mineralogical Magazine, vol. 75, 1833-1833.

Seifert T. & Pavlova G.G. (2016). New 40Ar/39Ar ages of Sn- and W-polymetallic mineralization in the Erzgebirge/Krusne hory (DE, CZ). Goldschmidt Conference Abstracts, 2792.

Schulmann K., Lexa O., Janousek V., Lardeaux J.-M. & Edel J.-B. (2014). Anatomy of a diffuse cryptic suture: An example from the Bohemian Massif, European Variscides. Geology vol. 42 (4), 275-278. https://doi.org/10.1130/G35290.1

Sharp W.D., Wenzel T., Nasdala L., Mertz D.F. & Becker T. (1997). Geochronology of Hercynian Meissen Massif magmatic rocks based on 40Ar/39Ar (amphibole, mica) and 206Pb/238U SHRIMP (zircon) data. Schriftenreihe Dt Geol Ges, vol. 2, 108-109.

Stampfli G.M. & Borel G.D. (2004). The TRANSMED Transects in Space and Time: Constraints on the Paleotectonic Evolution of the Mediterranean Domain. (*In*) Cavazza W., Roure F., Spakman W., Stampfli G.M., Ziegler P.A. (*eds*) The TRANSMED Atlas. The Mediterranean Region from Crust to Mantle. Springer, Berlin, Heidelberg. https://doi.org/10.1007/978-3-642-18919-7_3

Škácha P., Goliáš V., Sejkora J., Plášil J., Strnad L., Škoda R. & Ježek J. (2009). Hydrothermal uranium-base metal mineralization of the Jánská vein, Březové Hory, Příbram, Czech Republic: Lead isotopes and chemical dating of uraninite. J. Geosci. vol. 54, 1-13.

Štemprok M., Holub F.V. & Novák J.K. (2003). Multiple magmatic pulses of the Eastern Volcano-Plutonic Complex, Krušné hory/Erzgebirge batholith, and their phosphorus contents. Bulletin of Geosciences, vol. 78(3), 277-296.

Štemprok M. & Blecha V. (2015). Variscan Sn–W–Mo metallogeny in the gravity picture of the Krušné hory/Erzgebirge granite batholith (Central Europe). Ore Geology Reviews, vol. 69, 285-300. http://dx.doi.org/10.1016/j.oregeorev.2015.02.014

Swinkels L.J., Schulz-Isenbeck J., Frenzel M., Gutzmer J. & Burisch M. (2021) Spatial and Temporal Evolution of the Freiberg Epithermal Ag-Pb-Zn District, Germany. Economic Geology, vol. 116 (7), 1649-1667. https://doi.org/10.5382/econgeo.4833

Tichomirowa M. & Leonhardt D. (2010). New age determinations (Pb/Pb zircon evaporation, Rb/Sr) on the granites from Aue-Schwarzenberg and Eibenstock, Western Erzgebirge, Germany: Zeitschrift für Geologische Wissenschaften, vol. 38, 99-123.

Tichomirowa M., Käßner A., Sperner B., Lapp M., Leonhardt D., Linnemann U., Münker C., Ovtcharova M., Pfänder J.A., Schaltegger U., Sergeev S. & von Quadt A. (2019). Dating multiply overprinted granites: the effect of protracted magmatism and fluid flow on dating systems (zircon U-Pb: SHRIMP/SIMS, LA-ICP-MS, CA-IDTIMS; and Rb-Sr, Ar-Ar) – granites from the Western Erzgebirge. Chemical Geology, vol. 519, 11-38. https://doi.org/10.1016/j.chemgeo.2019.04.024

Tichomirowa M., Käßner A., Repstock A., Weber S., Gerdes A. & Whitehouse M. (2022). New CA-ID-TIMS U–Pb zircon ages for the Altenberg–Teplice Volcanic Complex (ATVC) document discrete and coeval pulses of Variscan magmatic activity in the Eastern Erzgebirge (Eastern Variscan Belt). Int J Earth Sci (Geol Rundsch), vol. 111, 1885-1908. https://doi.org/10.1007/s00531-022-02204-2

Tomek F., Žák J., Svojtka M., Finger F. & Waitzinger M. (2019). Emplacement dynamics of syn-collapse ring dikes: An example from the Altenberg-Teplice caldera, Bohemian Massif: Geological Society of America Bulletin, vol.131, 997-1016

Tomek F., Opluštil S., Svojtka M., Špillar V., Rapprich V. & Míková J. (2021). Altenberg–Teplice Caldera sourced Westphalian fall tuffs in the central and western Bohemian Carboniferous basins (eastern Variscan belt), International Geology Review, vol. 6(4), 441-468

Tugarinov A. I., Motorina Z. M., Naumov G. B., Sokolova N. T., Ermolaev N. P., Hodakovskij I. L., Mironova O. F. & Naumov V. B. (1970). Geochemische Bedingungen der Formierung der Uranvererzung in der Lagerstätte Schlema-Alberoda, Wismut GmbH.

Turnau E., Żelaźniewicz A. & Franke W. (2002). Middle to early late Viséan onset of late orogenic sedimentation in the Intra-Sudetic Basin, West Sudetes: miospore evidence and tectonic implication. Geologia Sudetica vol. 34, 9-16.

Turniak K., Mazur S., Domańska-Siuda J., Szuszkiewicz A. (2014). SHRIMP U–Pb zircon dating for granitoids from the Strzegom–Sobótka Massif, SW Poland: Constraints on the initial time of Permo-Mesozoic lithosphere thinning beneath Central Europe, Lithos vol. 208–209, 415-429. https://doi.org/10.1016/j.lithos.2014.09.031

von Seckendorff V., Timmerman M. J., Kramer W. & Wrobel P. (2004). New 40Ar/39Ar ages and geochemistry of late Carboniferous-early Permian lamprophyres and related volcanic rocks in the Saxothuringian Zone of the Variscan Orogen (Germany). (*In*) Wilson M., Neumann E.-R., Davies G.R., Timmerman M.J., Heeremans M. & Larsen B.T. (*eds*). Permo-Carboniferous magmatism and rifting in Europe, vol. 223, London, Geological society, 335-359.

Warkus F., Förster H.J. & Hansen B.T. (1998). New monazite U-Pb ages for granites from the Erzgebirge, Saxonia. Freiberger Forschungsheft, vol. C 471, 235-236.

Wendt I., Höhndorf A., Wendt J.I., Müller P. & Wetzel K. (1995). Radiometric dating of volcanic rocks in NW- Saxony by combined use of U-Pb and Sm-Nd zircon dating as well as Sm-Nd and Rb-Sr whole-rock and mineral systematics. Terra Nostra, vol. 7(95), 147-148.

Wenzel T., Mertz D.F., Oberhänsli R., Becker T. & Renne P.R. (1997). Age, geodynamic setting, and mantle enrichment processes of a K-rich intrusion from the Meissen massif northern Bohemian massif and implications for related occurrences from the mid-European Hercynian. Geol. Rundsch., vol. 86, 556-570.

Werner O. & Lippolt H.J. (1998). Datierung von postkinematischen magmatischen Intrusionsphasen des Erzgebirges: Thermische und hydrothermale Überprägung der Nebengesteine. Terra Nostra, vol. 98/2, 160-163.

Zhang R., Lehmann B., Seltmann R., Sun W. & Li C. (2017). Cassiterite U-Pb geochronology constrains magmatic-hydrothermal evolution in complex evolved granite systems: The classic Erzgebirge tin province (Saxony and Bohemia). Geology, vol. 45(12), 1095-1098. https://doi.org/10.1130/G39634.4

Zieger J., Bittner L., Gärtner A., Hofmann M., Gerdes A., Marko L. & Linnemann U. (2019). U–Pb ages of magmatic and detrital zircon of the Döhlen Basin: geological history of a Permian strike-slip basin in the Elbe Zone (Germany). International Journal of Earth Sciences, vol. 108, 887-910.

Zoubek V. (*Ed.*), Kodym O., Hoth K. & Lorenz W. (1996). Geological Map of the Czech Republic in scale of 1 : 200 000, Map of the Pre-Quaternary Formations, Sheet M-33-XIII Karlovy Vary – Plauen. Czech Geological Survey (in cooperation with Geologischer Dienst Freiberg), Prague, Czech Republic.

Žák J., Holub F.V. & Verner K. (2005). Tectonic evolution of a continental magmatic arc from transpression in the upper crust to exhumation of mid-crustal orogenic root recorded by episodically emplaced plutons: the Central Bohemian Plutonic Complex (Bohemian Massif). International Journal of Earth Sciences, vol. 94, 385-400.

Žák J., Verner K., Janoušek V., Holub F.V., Kachlík V., Finger F., Hajná J., Tomek F., Vondrovic L. & Trubač J. (2014). A plate-kinematic model for the assembly of the Bohemian Massif constrained by structural relationships around granitoid plutons. (*In*) Schulmann K., Oggiano G., Lardeaux J.M., Janoušek V. & Martínez Catalán J.R. (*eds*) The Variscan orogeny: extent, timescale and the formation of the European crust, vol 405. Geological Society, Special Publications, London, 169-196. https ://doi.org/10.1144/SP405 .9

7. Appendix 1

Compilation table of the ages available for magmatic, volcanic, sedimentary and ore deposit events. *For the confidence level, an age is considered “robust” if the method used is considered reliable in the geochronology community and provide a precise age (often with a rather small analytical error ≤5 Ma) with a good description of the sample’s mineralogy, geochemistry and location. Ages considered “passable” are determined by less precise method (e.g., Sm-Nd) which often give analytical error >5-10 Ma. A “Questionable” age is in contradiction with other geochronological study or petrographic/fieldwork observations.

Region	Sample	Type	Age	Error	Locality	Sublocality	Method	Remarks	Confidence level*	Reference
Early Permian & Carboniferous basins										
Döhlen Basin										
E. Erzgebirge	Unk2	Unkersdorf Tuff (Unkersdorf Formation)	294	3	Döhlen Basin	Freital (quarry Osterberg near the Weißeritz river)	U–Th–Pb LA-SF ICP-MS zircon	Concordia age (interpreted as the age of emplacement of the tuff by authors)	Robust	Zieger et al. (2019)
E. Erzgebirge	Unk1	Trachyandesite (Unkersdorf Formation)	293	5	Döhlen Basin	Freital (on top of the Burgwartsberg)	U–Th–Pb LA-SF ICP-MS zircon	Concordia age (interpreted as the cooling age by authors)	Robust	Zieger et al. (2019)
E. Erzgebirge	Ban4	Wachtelberg Ignimbrite (Upper Bannewitz Formation)	286	4	Döhlen Basin	Field between Freital and Cunnersdorf	U–Th–Pb LA-SF ICP-MS zircon	Concordia age	Robust	Zieger et al. (2019)
E. Erzgebirge	DB-1	Rhyodacitic lava (Unkersdorf Formation)	296	3	Döhlen Basin	Active quarry south of Wilsdruff	U-Pb SHRIMP zircon	12 zircons	Robust	Hoffmann et al. (2013)
E. Erzgebirge	DB-2	Rhyolitic Zauckerode Tuff, Niederhäslich	292	13	Döhlen Basin	Temporary outcrop in Freital	Pb/Pb single zircon evaporation age		Passable	Hoffmann et al. (2013)

Chemnitz basin										
E. & C. Erzgebirge		Zeisigwald Tuff pyroclastics	291	2	Chemnitz basin		U-Pb La-ICP-MS zircon		Robust	Luthardt et al. (2018)
E. & C. Erzgebirge	CB-1	Rhyolitic vitrophyric Planitz Ignimbrite (Planitz Formation)	296,6	3	Chemnitz basin, temporary outcrop in Zwickau	Planitz Formation	U-Pb SHRIMP zircon	14 zircons, Wetherhill graph	Robust	Hoffmann et al. (2013)
E. & C. Erzgebirge		Rhyolite dyke	278	5	St. Egidien and Chemnitz		$^{206}Pb/^{238}U$ SHRIMP zircon	interpreted as age of postkinematic Late Variscan volcanism in the Sub-Erzgebirge basin	Robust	Nasdala et al. (1998)
Kladno-Rakovník Basin										
E. Erzgebirge	25a	Tuff	297,16	0,17	Kladno-Rakovník Basin	Líne Formation	U-Pb CA-ID-TIMS zircon		Robust	Opluštil et al. (2016)
E. Erzgebirge	24	Clay horizon	298,97	0,09	Kladno-Rakovník Basin	Klobuky coal	U-Pb CA-ID-TIMS zircon		Robust	Opluštil et al. (2016)
E. Erzgebirge	16	Clay horizon	301,5	0,11	Kladno-Rakovník Basin	Kamínek	U-Pb CA-ID-TIMS zircon		Robust	Opluštil et al. (2016)
E. Erzgebirge	17a	Tuff	302,47	0,08	Kladno-Rakovník Basin	Mšec Member	U-Pb CA-ID-TIMS zircon		Robust	Opluštil et al. (2016)
E. Erzgebirge	11	Tuff	307,05	0,16	Kladno-Rakovník Basin	Nýřany Member	U-Pb CA-ID-TIMS zircon		Robust	Opluštil et al. (2016)
E. Erzgebirge	10	Tuff	312,36	0,07	Kladno-Rakovník Basin	Upper Radnice Member (Black Tuffite)	U-Pb CA-ID-TIMS zircon		Robust	Opluštil et al. (2016)
E. Erzgebirge	9	Tuff	312,38	0,05	Kladno-Rakovník Basin	Green Tuff	U-Pb CA-ID-TIMS zircon		Robust	Opluštil et al. (2016)

E. Erzgebirge	8	Tuff	313,22	0,04	Kladno-Rakovník Basin	Z-tuff	U-Pb CA-ID-TIMS zircon		Robust	Opluštil et al. (2016)
E. Erzgebirge	6	Tuff	313,2	0,06	Kladno-Rakovník Basin	Middle Volcanic Horizon	U-Pb CA-ID-TIMS zircon		Robust	Opluštil et al. (2016)
E. Erzgebirge	2	Tuff	313,41	0,07	Kladno-Rakovník Basin		U-Pb CA-ID-TIMS zircon		Robust	Opluštil et al. (2016)
E. Erzgebirge	4	Clay horizon	313,83	0,23	Kladno-Rakovník Basin	Velká Opuka	U-Pb CA-ID-TIMS zircon		Robust	Opluštil et al. (2016)
Pilsen Basin										
E. Erzgebirge	14	Tuff	303,73	0,13	Pilsen Basin	Týnec Formation	U-Pb CA-ID-TIMS zircon		Robust	Opluštil et al. (2016)
E. Erzgebirge	13	Clay horizon	305,99	0,07	Pilsen Basin		U-Pb CA-ID-TIMS zircon		Robust	Opluštil et al. (2016)
E. Erzgebirge	12	Clay horizon	308	0,04	Pilsen Basin		U-Pb CA-ID-TIMS zircon		Robust	Opluštil et al. (2016)
Radnice Basin										
E. Erzgebirge	3	Ash bed	314,36	0,09	Radnice Basin		U-Pb CA-ID-TIMS zircon		Robust	Opluštil et al. (2016)
C. Erzgebirge	BOB-1	Rhyolitic ? (Olbernhau Formation)	302,6	2,8	Fallout deposit (rhyolitic?) (Drilling B6/99, 13.15–13.25 m depth)		U-Pb SHRIMP zircon	7 zircons	Robust	Hoffmann et al. (2013)
North Saxon Volcanic Complex										
E. Erzgebirge		Distal tuff	298,3	9,1		Kohren formation/ Flechtingen	Pb/U SHRIMP on zircon		Passable	Hoffmann et al. (2013)
E. Erzgebirge		Ignimbrite	294,4	1,8		Rochlitz ignimbrite	Pb/U SHRIMP on zircon		Robust	Hoffmann et al. (2013)
E. Erzgebirge		Ignimbrite	285,6	1,1		Wurzen Volcanic System	U-Pb on zircon		Robust	Wendt et al. (1995)

E. Erzgebirge		Ignimbrite	284	11		Wurzen Volcanic System	Sm/Nd whole rock	Passable	Wendt et al. (1995)
E. Erzgebirge		Ignimbrite	287	5		Wurzen Volcanic System	Rb/Sr	Robust	Wendt et al. (1995)
E. Erzgebirge		Rhyolite	289,3	4,1		Wurzen Volcanic System	Pb/U SHRIMP on zircon	Robust	Hoffmann et al. (2013)
E. Erzgebirge		Rhyolite	290,2	4,1		Wurzen Volcanic System	Pb/U SHRIMP on zircon	Robust	Hoffmann et al. (2013)
Freiberg district dykes									
E. Erzgebirge		Rhyolite	~300	n.d.		Rhyolite dyke	U-Pb CA-ID-TIMS on zircon		Tichomirowa et al. (personal communication)
Epithermal vein									
E. Erzgebirge		Ag-Pb-Zn epithermal vein	276	16	Freiberg		Rb-Sr isotopes sphalerite	Questionable	Ostendorf et al. (2019)
Skarn									
E. Erzgebirge		Skarn	304,9	3,2	Berggießh übel		U-Pb La-ICP-MS garnet	Robust	Burisch et al. (2019a)
E. Erzgebirge		Skarn	301,5	5,7	Berggießh übel		U-Pb La-ICP-MS garnet	Robust	Burisch et al. (2019a)
Younger granite									
E. Erzgebirge		Granite	302	4	Seiffen		Th-U-Pb monazite	Robust	Förster and Rhede (2006)
E. Erzgebirge		Granite	301	5	Seiffen		K-Ar siderite	Robust	Förster and Rhede (2006)
Oederan Forest Volcano									
E. Erzgebirge	MfNC-2014-01	Ignimbrite	309,4	2,6	Oederan Forest Volcano		U-Pb LA-ICP-MS zircon	Robust	Löcse et al. (2019)
E. Erzgebirge	MfNC-2014-02	Ignimbrite	309	1,8	Oederan Forest Volcano		U-Pb LA-ICP-MS zircon	Robust	Löcse et al. (2019)
E. Erzgebirge	MfNC-2014-05	Schweddey ignimbrite	310,4	1,6	Schwedde y		U-Pb LA-ICP-MS zircon	Robust	Löcse et al. (2019)

E. Erzgebirge	MfNC-2014-08	Schweddey ignimbrite	310,1	2	Schweddey	U-Pb LA-ICP-MS zircon		Robust	Löcse et al. (2019)
E. Erzgebirge	MfNC-2014-11	Roter Stein dyke	311,4	2,7	Roter Stein	U-Pb LA-ICP-MS zircon		Robust	Löcse et al. (2019)
E. Erzgebirge	MfNC-2014-12	Metzdorf dyke	298,6	2,5	Metzdorf	U-Pb LA-ICP-MS zircon		Robust	Löcse et al. (2019)
Flöha basin									
E. Erzgebirge		Flöha ignimbrite	311,8	9,4	Flöha ignimbrite	U-Pb LA-ICP-MS zircon		Robust/passable	Löcse et al. (2019)
E. Erzgebirge		Flöha ignimbrite	309,2	3,8	Flöha ignimbrite	U-Pb LA-ICP-MS zircon		Robust	Löcse et al. (2019)
Greisen									
Altenberg									
E. Erzgebirge	ALT-1	Greisen(?)	321,4	3,3	Altenberg	U-Pb LA-ICP-MS cassiterite		Questionable	Zhang et al. (2017)
E. Erzgebirge	ALT-2	Greisen(?)	322,4	2,8	Altenberg	U-Pb LA-ICP-MS cassiterite		Questionable	Zhang et al. (2017)
E. Erzgebirge	5000	Greisen (metamonzogranite greisenized)	323,9	2,5	Altenberg	Re-Os molybdenite		Questionable	Romer et al. (2007)
E. Erzgebirge	TS 1	Quartz vein	317,9	2,4	Altenberg	Re-Os molybdenite		Robust	Romer et al. (2007)
E. Erzgebirge		Granite?	318	2	Altenberg	Re-Os molybdenite		Questionable	Romer et al. (2007)
E. Erzgebirge		Granite?	324	2	Altenberg	Re-Os molybdenite		Questionable	Romer et al. (2007)
E. Erzgebirge		Granite	327	4	Markersbach	U-Pb LA-ICP-MS monazite, xenotime, uraninite		Questionable	Hofmann et al. (2009)
E. Erzgebirge	Gal 20-39	Granite	305	3	Altenberg	Rb-Sr whole-rock	lowered isochron age	Questionable	Gerstenberger (1989)
E. Erzgebirge		Granite	293	n.d.	Altenberg	Rb-Sr whole-rock	Error not available	Robust	Haack (1990)
Krupka									

E. Erzgebirge	KP-1	Greisen	320,1	2,8	Krupka	U-Pb LA-ICP-MS cassiterite		Questionable	Zhang et al. (2017)
E. Erzgebirge	greisen	Greisen	312	3,1	Krupka-Knötel	$^{40}Ar/^{39}Ar$ Li-mica (protolithionite)		Robust	Seifert and Pavlova (2016)
E. Erzgebirge	51/M	Quartz vein within greisen (metamonzogranite greisenized)	319,2	2	Krupka-Knötel	Re-Os molybdenite		Robust	Ackerman et al. (2017)
E. Erzgebirge	51/M	Quartz vein within greisen (metamonzogranite greisenized)	317,7	2	Krupka-Knötel	Re-Os molybdenite		Robust	Ackerman et al. (2017)
E. Erzgebirge	Kru-2	Quartz vein within greisen (metamonzogranite greisenized)	315,3	2,3	Krupka-Preisselberg	Re-Os molybdenite		Robust	Ackerman et al. (2017)
Zinnwald/Cínovec									
E. Erzgebirge		Massive greisen, greisen veins, non greisenised	312,8	1,8	Zinnwald/ Cínovec	$^{40}Ar/^{39}Ar$ Li-mica (zinnwaldite)	average inverse isochron age; interpretated by authors as a minimum age for greisenisation	Robust	Neßler et al. (2016)
E. Erzgebirge	Cin-9	Quartz vein within greisen (meta-albite granite greisenized)	322,4	5,5	Zinnwald	Re-Os molybdenite		Questionable	Ackerman et al. (2017)
E. Erzgebirge	ZW-1	Greisen	321,6	3,1	Zinnwald	U-Pb LA-ICP-MS cassiterite		Questionable	Zhang et al. (2017)
E. Erzgebirge	N.A.	Greisen	312,6	2,1	Zinnwald	Ar-Ar Li-mica		Robust	Seifert et al. (2011)
E. Erzgebirge	N.A.	Greisen	314,9	2,3	Zinnwald	Ar-Ar Li-mica		Robust	Seifert et al. (2011)
E. Erzgebirge		Greisen (meta albite granite greisenized)	314,1	1,5	Zinnwald	Ar-Ar zinnwaldite		Robust	Atanasova (2012)

E. Erzgebirge		Granite	309	3	Zinnwald	protholitionite granite	K-Ar in Li-mica	recalculated age no errors given	Robust	Dolejš and Štemprok (2001)
E. Erzgebirge		Greisen	311,4	3	Zinnwald		$^{40}Ar/^{39}Ar$ Li-mica (zinnwaldite)	Li-Sn-W deposit	Robust	Seifert and Pavlova (2016)
E. Erzgebirge		Greisen (vein)	312,5	3,1	Zinnwald		$^{40}Ar/^{39}Ar$ Li-mica (zinnwaldite)		Robust	Seifert and Pavlova (2016)
E. Erzgebirge		Greisen (albite granite)	321	22	Zinnwald	Cínovec+Sachsen höhe	Sm-Nd fluorite		Passable	Höhndorf et al. (1994)
Sadisdorf										
E. Erzgebirge	Sad-6	Greisen (meta albite granite greisenized)	321,4	3,8	Sadisdorf		Re-Os molybdenite		Questionable	Ackerman et al. (2017)
E. Erzgebirge	SD-1	Greisen/vein	326,1	3,4	Sadisdorf		U-Pb LA-ICP-MS cassiterite		Questionable	Zhang et al. (2017)
E. Erzgebirge		Mica-quartz-topaz greisen (“Innengreisen”), (meta albite granite greisenized)	310	3,5	Sadisdorf	Sn(-W-Mo-Cu-Zn-In) deposit	$^{40}Ar/^{39}Ar$ Li-mica (protolithionite)		Robust	Seifert and Pavlova (2016)
E. Erzgebirge		Meta albite granite greisenized	326	8	Sadisdorf		Sm/Nd wolframite		Questionable	Kempe and Belyatsky (1997)
Lamprophyres										
C. Erzgebirge		Minette dike (Lp)	316	3	Griesbach (SW Zschopau)		$^{40}Ar/^{39}Ar$ biotite		Robust	von Seckendorff et al. (2004)
C. Erzgebirge		Kersantite dike (Lp)	319	3	Scharfenstein (SE Chemnitz)		$^{40}Ar/^{39}Ar$ biotite		Robust	von Seckendorff et al. (2004)
E. Erzgebirge		Minette dike (Lp)	320	3	St. Michaelis (Brand-Erbisdorf)		$^{40}Ar/^{39}Ar$ biotite		Robust	von Seckendorff et al. (2004)
E. Erzgebirge		Kersantite dike (Lp)	324	3	Rabenau (S Dresden)		$^{40}Ar/^{39}Ar$ biotite		Robust	von Seckendorff et al. (2004)

E. Erzgebirge		Meta albite granite greisenized	313,04	0,67	Sadisdorf	U-Pb LA-ICP-MS cassiterite	Robust	Leopardi et al. (submitted)
				Altenberg-Teplice caldera				
Altenberg ring dikes								
E. Erzgebirge	FT13	Microgranite	312	3	Altenberg-Frauenstein microgranite	U-Pb LA-ICP-MS zircon	Robust	Tomek et al. (2019)
E. Erzgebirge	FT63	Microgranite	312	4	Altenberg-Frauenstein microgranite	U-Pb LA-ICP-MS zircon	Robust	Tomek et al. (2019)
E. Erzgebirge	FT153	Microgranite	312	3	Altenberg-Frauenstein microgranite	U-Pb LA-ICP-MS zircon	Robust	Tomek et al. (2019)
E. Erzgebirge	19Elend	Microgranite	313,1	0,5	Altenberg-Frauenstein microgranite	U-Pb CA-ID-TIMS zircon	Robust	Tichomirowa et al. (2022)
E. Erzgebirge	Frau	Microgranite	314,3	0,4	Altenberg-Frauenstein microgranite	U-Pb CA-ID-TIMS zircon	Robust	Tichomirowa et al. (2022)
E. Erzgebirge		Microgranite	319,2	2,4	Altenberg-Frauenstein microgranite	U/Pb evaporation zircon	Robust	Romer et al. (2010)
E. Erzgebirge	GP	Microgranite	297	13	Altenberg-Frauenstein microgranite	K-Ar amphibole	Passable	Müller et al. (2005)

E. Erzgebirge		Microgranite	307-309	n.d.	Altenberg-Frauenstein microgranite		$^{40}Ar/^{39}Ar$ biotite, hornblende		Robust	Seltmann and Schilka (1995)
		Microgranite	300-290	n.d.	Altenberg-Frauenstein microgranite		$^{40}Ar/^{39}Ar$ K-feldspar		Questionable	Seltmann and Schilka (1995)
E. Erzgebirge		Microgranite (granite porphyry)	290	5	Altenberg-Frauenstein microgranite		$^{207}Pb/^{206}Pb$ evaporation zircon	Interpreted by authors as the age of greisenization and Sn mineralization	Questionable	Kempe et al. (1999)
E. Erzgebirge		Microgranite (granite porphyry)	333	8	Altenberg-Frauenstein microgranite		$^{207}Pb/^{206}Pb$ evaporation zircon	Interpreted by authors as the age of the Atenberg microgranite emplacement	Questionable	Kempe et al. (1999)
Sayda-Berggießhübel Dike Swarm										
E. Erzgebirge	19Biene	Rhyolitic dike	310,9	0,5	Sayda-Berggießhübel dyke swarm	3. phase	U-Pb CA-ID-TIMS zircon		Robust	Tichomirowa et al. (2022)
E. Erzgebirge	19Turm	Rhyolitic dike	313,8	4,9	Sayda-Berggießhübel dyke swarm	Frauenstein?	U-Pb CA-ID-TIMS zircon		Robust	Tichomirowa et al. (2022)
E. Erzgebirge	FT168	Rhyolitic dike	314	4	Sayda-Berggießhübel dyke swarm		U-Pb LA-ICP-MS zircon	concordia age	Robust	Tomek et al. (2021)
E. Erzgebirge	FT170	Pyroclastic dike	313	3	Sayda-Berggießhübel dyke swarm		U-Pb LA-ICP-MS zircon	concordia age	Robust	Tomek et al. (2021)
E. Erzgebirge	FT168	Rhyolite	314	4	Sayda-Berggießh		U-Pb LA-ICP-MS zircon	concordia age	Robust	Tomek et al. (2021)

					übel dyke swarm					
Teplice ignimbrite										
E. Erzgebirge	TAVC-2	Ignimbrite	308,8	4,9	Teplice ignimbrite		U-Pb SHRIMP zircon	Wetherhill graph	Passable	Hoffmann et al. (2013)
E. Erzgebirge	Sö30	Ignimbrite	314,2	0,4	Teplice ignimbrite	Teichweg member	U-Pb CA-ID-TIMS zircon		Robust	Tichomirowa et al. (2022)
E. Erzgebirge	19Hart	Ignimbrite	314,1	0,4	Teplice ignimbrite	Lugstein-Pramenáč	U-Pb CA-ID-TIMS zircon		Robust	Tichomirowa et al. (2022)
E. Erzgebirge	19Lug	Ignimbrite	314,2	0,5	Teplice ignimbrite	Lugstein-Pramenáč	U-Pb CA-ID-TIMS zircon		Robust	Tichomirowa et al. (2022)
E. Erzgebirge	2055-85	Ignimbrite	323	2	Teplice ignimbrite	Teichweg member	U-Pb LA-ICP-MS zircon	concordia age	Questionable	Casas-García et al. (2019)
E. Erzgebirge	HS-01	Ignimbrite	313	3	Teplice ignimbrite	Teichweg member	U-Pb LA-ICP-MS zircon	concordia age	Robust	Casas-García et al. (2019)
E. Erzgebirge	TR-22	Ignimbrite	310	4	Teplice ignimbrite	Lugstein-Pramenáč	U-Pb LA-ICP-MS zircon	concordia age	Questionable	Casas-García et al. (2019)
E. Erzgebirge	TR-39	Ignimbrite	313	5	Teplice ignimbrite	Vlčí kámen-Medvědí vrch Member.	U-Pb LA-ICP-MS zircon	concordia age core	Robust	Casas-García et al. (2019)
E. Erzgebirge	TR-39	Ignimbrite	304	5	Teplice ignimbrite	Medvědí vrch	U-Pb LA-ICP-MS zircon	concordia age rim	Questionable	Casas-García et al. (2019)
E. Erzgebirge	TR-19	Ignimbrite	312	4	Teplice ignimbrite	Přední Cínovec member	U-Pb LA-ICP-MS zircon	concordia age	Robust	Casas-García et al. (2019)
E. Erzgebirge	FT164	Ignimbrite	314	3	Teplice ignimbrite	extra caldera facies	U-Pb LA-ICP-MS zircon	concordia age	Robust	Tomek et al. (2021)
E. Erzgebirge	FT164	Ignimbrite	314	3	Teplice ignimbrite	Přední Cínovec member	U-Pb LA-ICP-MS zircon	concordia age	Robust	Tomek et al. (2021)
Schönfeld complex										
E. Erzgebirge	19Schön	Ignimbrite	322,1	0,4	Schönfeld		U-Pb CA-ID-TIMS zircon		Robust	Tichomirowa et al. (2022)
E. Erzgebirge	SBR	Rhyolite	300	11	Schönfeld	Schönfeld basal rhyolite	K-Ar biotite		Passable	Müller et al. (2005)
E. Erzgebirge	TAVC-1	Rhyolitic Mikulov Ignimbrite	326,8	4,3	Schönfeld	Mikulov Beds	U-Pb SHRIMP zircon	Wetherhill graph	Robust	Hoffmann et al. (2013)

					Tharandt Forest Caldera					
E. Erzgebirge	Grund	Ignimbrite	311,9	0,4	Tharand Forest Caldera		U-Pb CA-ID-TIMS zircon		Robust	Breitkreuz et al. (2021)
E. Erzgebirge	99-103	Ignimbrite	313,4	0,4	Tharand Forest Caldera		U-Pb CA-ID-TIMS zircon		Robust	Breitkreuz et al. (2021)
E. Erzgebirge	99-63	Rhyolite	314,5	0,5	Tharand Forest Caldera	Outer ring dike	U-Pb CA-ID-TIMS zircon		Robust	Breitkreuz et al. (2021)
					Meißen volcanic complex					
E. Erzgebirge	MVC-1	Ignimbrite	302,9	2,5	Meißen massif	Rhyodacitic Leutewitz Ignimbrite	U-Pb SHRIMP zircon	2 zircons	Passable	Hoffmann et al. (2013)
					Pre-caldera Plutons					
E. Erzgebirge	Nbg 1	Granite	318,2	0,5	Niedebobrisch		U-Pb CA-ID-TIMS zircon		Robust	Breitkreuz et al (2021)
E. Erzgebirge	Nbg 2	Granite	319,5	0,4	Niedebobrisch		U-Pb CA-ID-TIMS zircon		Robust	Breitkreuz et al (2021)
E. Erzgebirge		Granite	324	4	Niedebobrisch		U-Pb dating by isotope dilution-thermal ion mass spectrometry monazite, xenotime, uraninite		Passable	Förster et al. (1998)
E. Erzgebirge		Granite	320	6	Niedebobrisch		Pb/Pb evaporation zircon		Passable	Tichomirowa (1997)
E. Erzgebirge	FLG01	Monzogranite	319	2	Fláje		U-Pb LA-ICP-MS zircon	concordia age	Robust	Tomek et al. (2021)
E. Erzgebirge	FT163	Monzogranite	326,8	4,3	Fláje		U-Pb LA-ICP-MS zircon	concordia age	Robust	Tomek et al. (2021)
E. Erzgebirge	FLG01	Monzogranite	319	2	Fláje		U-Pb LA-ICP-MS zircon	concordia age	Robust	Tomek et al. (2021)
E. Erzgebirge	FT163	Monzogranite	325	3	Fláje		U-Pb LA-ICP-MS zircon	concordia age	Robust	Tomek et al. (2021)
E. Erzgebirge		Pluton	326	6	Leuben		U-Pb SHRIMP zircon		Passable	Nasdala et al. (1999)

E. Erzgebirge		Pluton	330	5	Heidenschanze		U-Pb SHRIMP zircon	Passable	Nasdala et al. (1999)
E. Erzgebirge		Pluton	330,4	2,8	Leuben		Ar-Ar amphibole	Robust	Wenzel et al. (1997)
E. Erzgebirge		Pluton	329,1	2,8	Heidenschanze		Ar-Ar amphibole	Robust	Wenzel et al. (1997)
E. Erzgebirge		Pluton	323,4	1	Hauptgranite		?	Robust	Sharp et al. (1997) in Müller (2011)
E. Erzgebirge		Pluton	323,6	1	Riesensteingranit		?	Robust	Sharp et al. (1997) in Müller (2011)
Central Erzgebirge Plutons									
C. Erzgebirge		Greifenstein granite	323,9	3,5	Ehrenfriedersdorf		$^{206}Pb/^{238}U$ ID TIMS (dating by isotope dilution-thermal ion mass spectrometry) uraninite	Robust	Romer et al. (2007)
C. Erzgebirge	Q8	Sauberg stockscheider (marginal flat-lying pegmatite) aplite	320,6	1,9	Ehrenfriedersdorf	Sauberg mine	$^{206}Pb/^{238}U$ ID TIMS uraninite (representing a melt pocket)	Robust	Romer et al. (2007)
C. Erzgebirge		Sauberg stockscheider (marginal flat-lying pegmatite) aplite	319,7	3,4	Ehrenfriedersdorf	Sauberg mine	Th-U-Pb uraninite	Robust	Romer et al. (2007)
C. Erzgebirge		Granite	323,9	2,9	Ehrenfriedersdorf		U-Pb hydrothermal apatite	Robust	Romer et al. (2007)
C. Erzgebirge	E1 + E2	Granite	317,6	1,6	Ehrenfriedersdorf	Sauberg mine	U-Pb hydrothermal apatite	Robust	Romer et al. (2007)
C. Erzgebirge		Ehrenfriedersdorf granite	322	5	Ehrenfriedersdorf		Pb/Pb zircon	Robust	Seifert (2008)
C.Erzgebire		Erhenfriedersdorf granite	324-317	n.d.	Ehrenfriedersdorf		U/Pb apatite	Robust	Romer et al. (2007)
C. Erzgebirge		Ehrenfriedersdorf granite	310,8	1,1	Ehrenfriedersdorf		Ar/Ar muscovite	Robust	Werner and Lippolt (1998)
C. Erzgebirge		Pobershau granite	321	3	Pobershau		U/Pb ID TIMS monazite	Robust	Warkus et al. (1998)

C. Erzgebirge		Pobershau g ranite	317	2	Pobershau	U/Pb monazite, xenotime, uraninite		Robust	Förster (1998)
C. Erzgebirge		Hora Svaté Kateřiny granite	308	14		Th-U-Pb monazite		Passable	Breiter (2008)
West Erzgebirge Plutons									
W. Erzgebirge	ASB 665	Aue granite	324,3	5,5		U-Pb LA-ICP-MS on zircon	$^{206}Pb/^{238}U$ weighted mean	Robust	Tichomirowa et al. (2019)
W. Erzgebirge		Aue granite	328,6	2	Aue	Pb/Pb evaporation zircon		Robust	Tichomirowa and Leonhardt (2010)
W. Erzgebirge		Schalenberg granite	325,7	7	Lauter	Pb/Pb evaporation zircon		Robust	Tichomirowa and Leonhardt (2010)
W. Erzgebirge	ASB 668	Lauter granite	326,8	3,6		U-Pb LA-ICP-MS on zircon	$^{206}Pb/^{238}U$ weighted mean	Robust	Tichomirowa et al. (2019)
W. Erzgebirge		Lauter granite	331	2,9	Lauter	Pb/Pb evaporation zircon		Robust	Tichomirowa and Leonhardt (2010)
W. Erzgebirge		Abertamy granite	322,8	3,5		Pb/Pb evaporation zircon		Robust	Kovarikova et al. (2007)
W. Erzgebirge	BER 788	Bergen granite	315,8	3,7	Quarry Streuberg	U-Pb LA-ICP-MS on zircon	$^{206}Pb/^{238}U$ weighted mean	Robust	Tichomirowa et al. (2019)
W. Erzgebirge	BER 789	Bergen granite	321,1	3,7	Quarry NW Trieb	U-Pb LA-ICP-MS on zircon	$^{206}Pb/^{238}U$ weighted mean	Robust	Tichomirowa et al. (2019)
W. Erzgebirge	BER79 0	Bergen granite	330,3	3,8	Quarry SE Trieb	U-Pb LA-ICP-MS on zircon	$^{206}Pb/^{238}U$ weighted mean	Robust	Tichomirowa et al. (2019)
W. Erzgebirge	BER 791	Bergen granite	325,2	4,3	Quarry Kuxenberg h	U-Pb LA-ICP-MS on zircon	$^{206}Pb/^{238}U$ weighted mean	Robust	Tichomirowa et al. (2019)
W. Erzgebirge		Bergen granite	323	2	Bergen	U/Pb monazite, xenotime, uraninite		Robust	Förster (1998)
W. Erzgebirge		Kirchberg granite	324	5	Kirchberg	U/Pb monazite, xenotime, uraninite		Robust	Förster (1998)
W. Erzgebirge		Kirchberg granite	330	5	Kirchberg	Th-U-Pb uraninite		Robust	Kempe (2003)
W. Erzgebirge		Auerhammer granite	322	6		U-Pb ID TIMS monazite		Passable	Warkus et al. (1998)
W. Erzgebirge	EIB 710	Eibenstock granite	315,1	1,0	Kamelfelse n	40Ar-39Ar on Li-mica		Robust	Tichomirowa et al. (2019)

W. Erzgebirge		Eibenstock granite	319,8	1	Eibenstock	Pb/Pb evaporation zircon		Robust	Tichomirowa and Leonhardt (2010)
W. Erzgebirge		Eibenstock granite	316	3	Eibenstock	U-Pb monazite, xenotime, uraninite		Robust	Förster (1998)
W. Erzgebirge		Eibenstock granite	321	4	Eibenstock	U-Pb monazite		Robust	Warkus et al. (1998)
W. Erzgebirge		Eibenstock granite	320	8	Eibenstock	Pb/Pb evaporation zircon		Robust	Kempe et al. (2004)
W. Erzgebirge		Eibenstock granite	322	3	Gottesberg	U/Pb SHRIMP		Robust	Seifert (2008)
W. Erzgebirge		Eibenstock granite	325	3,7	Gottesberg	Pb/Pb		Robust	Seifert (2008)
W. Erzgebirge		Blauenthal granite	315	10		Pb/Pb evaporation zircon		Robust	Tichomirowa and Leonhardt (2010)
W. Erzgebirge		Walfischkopf granite	314,7	4,3		Pb/Pb evaporation zircon		Robust	Tichomirowa and Leonhardt (2010)
W. Erzgebirge		Krinitzberg granite	318,8	2,9		Pb/Pb evaporation zircon		Robust	Tichomirowa and Leonhardt (2010)
W. Erzgebirge		Rhyolite dyke in Gottesberg granite	304-290	n.d.	Eibenstock	U/Pb, K/Ar monazite, biotite		Robust	Förster et al. (2007)
W. Erzgebirge		Rhyolite dyke in Eibenstock	290	5	Eibenstock	Pb/Pb evaporation zircon		Robust	Kempe et al. (2004)
W. Erzgebirge		Rhyolite dyke in Eibenstock	297	8	Eibenstock	U/Pb SHRIMP zircon		Robust	Kempe et al. (2004)
W. Erzgebirge		Microgranite in Eibenstock granite	312,5	4,6	Gottesberg	Pb/Pb evaporation zircon		Robust	Seifert (2008)
W. Erzgebirge	ASB 670	Schwarzenberg granite	322,0	1,4	Schwarzen berg	U-Pb CA-ID-TIMS on zircon	Concordia age	Robust	Tichomirowa et al. (2019)